Acta Biotheoretica (2023) 71:19
https://doi.org/10.1007/s10441-023-09470-w

REGULAR ARTICLE

Assessment of the Global Variance Effective Size of Subdivided Populations, and Its Relation to Other Effective Sizes

Ola Hössjer[1] · **Linda Laikre**[2] · **Nils Ryman**[2]

Received: 8 November 2021 / Accepted: 28 June 2023 / Published online: 17 July 2023

Abstract

The variance effective population size (N_{eV}) is frequently used to quantify the expected rate at which a population's allele frequencies change over time. The purpose of this paper is to find expressions for the global N_{eV} of a spatially structured population that are of interest for conservation of species. Since N_{eV} depends on allele frequency change, we start by dividing the cause of allele frequency change into genetic drift within subpopulations (*I*) and a second component mainly due to migration between subpopulations (*II*). We investigate in detail how these two components depend on the way in which subpopulations are weighted as well as their dependence on parameters of the model such a migration rates, and local effective and census sizes. It is shown that under certain conditions the impact of *II* is eliminated, and N_{eV} of the metapopulation is maximized, when subpopulations are weighted proportionally to their long term reproductive contributions. This maximal N_{eV} is the sought for global effective size, since it approximates the gene diversity effective size N_{eGD}, a quantifier of the rate of loss of genetic diversity that is relevant for conservation of species and populations. We also propose two novel versions of N_{eV}, one of which (the backward version of N_{eV}) is most stable, exists for most populations, and is closer to N_{eGD} than the classical notion of N_{eV}. Expressions for the optimal length of the time interval for measuring genetic change are developed, that make it possible to estimate any version of N_{eV} with maximal accuracy.

Keywords Genetic diversity · Length of time interval · Matrix analytic recursions · Metapopulation · Migration–drift equilibrium · Perturbation theory of matrices · Variance effective size

Mathematics Subject Classification 60J28 · 92D10 · 92D15 · 92D20

Extended author information available on the last page of the article

1 Introduction

1.1 Background on Effective Population Sizes

The effective population size N_e is a well known concept (Wright 1931, 1938) that quantifies the rate at which genetic variation of a population is lost over time. This is important in conservation biology, where retention of sufficient levels of genetic diversity to allow adaptation to changing environmental conditions is of major concern for the long term viability and conservation of species and populations (Frankham et al. 2010; Traill et al. 2010; Hoban et al. 2021; Allendorf et al. 2022). Since many populations exhibit some type of geographic substructure, it is crucial to assess in which way and how much this impacts N_e. Typically, such a structure is modelled as a metapopulation that consists of a number of more or less connected subpopulations. For short term conservation of species it is mainly genetic drift within and migration between subpopulations that impact N_e, whereas mutation and natural selection are usually ignored.

Many versions of effective size have been proposed, as recently discussed by Gilbert and Whitlock (2015), Wang (2016), Waples (2016), Ryman et al. (2019), and Nadachowska-Brzyska et al. (2022). In this paper we focus on the variance effective size N_{eV} (Crow 1954), where loss of genetic variation is quantified in terms of the variance of frequency change of genetic variants (alleles). If genetic data is available from at least two points in time, the temporal method (Kimbras and Tsakas 1971; Nei and Tajima 1981; Pollack 1983; Waples 1989; Jorde and Ryman 2007) can be employed to estimate N_{eV}. For this reason N_{eV} is one of the most frequently used notions of effective size that is recommended because it is multigenerational (Frankham et al. 2019; Frankham 2021). On the other hand, N_{eV} is typically *not* the best effective size for assessing the rate at which genetic diversity is lost in substructured populations. Since this rate is an important criterion for conservation of species, this is potentially a drawback of N_{eV} (Ryman et al. 2019).

In order to find out whether versions of N_{eV} for substructured populations exist that are more appropriate for estimating N_e for conservation purposes, a first step is to understand how various parameters of a population genetic model influence N_{eV}. To this end, it is important to build a mathematical framework for how the genetic makeup of a population evolves over time, and then find expressions for the variance of allele frequency change. Using such an approach, Whitlock and Barton (1997) noted that N_{eV} is a function of several parameters, such as the local effective sizes of subpopulations under isolation, the migration pattern between subpopulations and the way in which subpopulations are weighted in order for N_{eV} to reflect, for instance, local or global aspects of the variance effective size. Hössjer et al. (2014) added local census sizes to the model and considered subpopulation weights of general form. Hössjer et al. (2016) noticed that previous analyses of N_{eV} had been overly simplistic and neglected the impact of subpopulation differentiation at the first time point at which genetic data is collected.

1.2 Objectives

The purpose of this paper is to find versions of N_{eV} for the metapopulation that are of interest for conservation, by appropriately quantifying the rate of loss of genetic diversity. To this end, we will generalize work of Whitlock and Barton (1997), Ryman et al. (2014) and Hössjer et al. (2014, 2016) and study the variance effective size of structured populations by means of matrix analytic methods, where standardized covariances of allele frequency change and gene diversities (Nei 1973) are updated recursively over time. More specifically we consider three aspects of N_{eV}: (i) A careful analysis of allele frequency change and subpopulation weights, which will lead us to a version of N_{eV} that is of interest for conservation, (ii) Introduction of two novel and more stable ways of defining N_{eV}, both of which have versions that are of relevance for conservation, (iii) Finding expressions for the length of the interval between the two time points at which genetic data is collected, which is optimal in terms of estimating N_{eV} with maximal accuracy. In the rest of this section, we describe these three steps in more detail.

For the first contribution (i), following Hössjer et al. (2016) we divide expected squared allele frequency change between the two time points at which genetic data is collected into two components I and II, and study conditions under which the impact of II is negligible. In order to motivate more closely this first aspect of our article, we will start by explaining the meaning of these two terms I and II.

The first component I was analyzed by Whitlock and Barton (1997) and Hössjer et al. (2014), and it quantifies how much standardized covariances of allele frequency change increase or how much the gene diversity decreases between the two time points at which genetic data is collected. We will refer to I as the drift term, since it is mainly genetic drift that causes loss of genetic variation, and for this reason I is usually the most important source of genetic change. Indeed, gene diversity decrease I is equivalent to gene identity increase, a haploid approximation of increased inbreeding that is of major concern for short term protection of species (Franklin 1980; Jamieson and Allendorf 2012). For this reason the gene diversity effective size N_{eGD} is of interest for conservation since it only involves the genetic drift term I but not the other term II. N_{eGD} is however of more relevance for long term than for short term conservation since it approximates the additive genetic variance effective size N_{eAV} (Franklin 1980; Hössjer et al. 2016). This is important since the frequently used conservation guideline for long term survival, that stipulates that N_e should be larger than 500 (Franklin 1980; Jamieson and Allendorf 2012) or larger than 1000 (Frankham et al. 2014; Pérez-Pereira et al. 2022), relates to N_{eAV} (Ryman et al. 2019). However, since N_{eGD} (and N_{eAV}) is difficult to estimate in practice, it is important to assess how well it is approximated by N_{eV}.

The second term II was introduced in Hössjer et al. (2016) and it quantifies how much allele frequency change in the past, before the first time point when data is collected, is correlated with allele frequency change between the two time points of data collection, with a negative correlation corresponding to a positive value of II. We could therefore refer to $-II$ as a correlation between allele frequency change of the past and the present. But since II vanishes when all subpopulations are isolated and additionally the same subpopulation weights are used at the two time points at

which genetic data is collected, it follows that II is mainly caused by migration. For this reason we will speak of II as a migration or gene flow term. It is also the case that II is present only when there is subpopulation differentiation at the first time point of data collection.

In order to shed further light on the relation between N_{eGD} and N_{eV}, we continue the analysis of Hössjer et al. (2016) and express genetic drift I and gene flow II in terms of how subpopulations are weighted, and also in terms of parameters of the population genetic model such as the local census and effective sizes and the migration rates between subpopulations. In particular, we demonstrate that II is highly dependent on local census sizes, whereas I is virtually independent of them (although local census sizes were introduced in Hössjer et al. (2014), they had little impact on N_{eV} since II was not included as a component of allele frequency change in that article).

It is of particular interest to find conditions under which it is possible to estimate N_{eV} in such a way that II is eliminated. It was shown in Hössjer et al. (2016) that the gene flow contribution II to the variance effective size vanishes when subpopulations are weighted proportionally to their long term reproductive contribution (Hill 1972; Nagylaki 1980; Whitlock and Barton 1997). This means that each subpopulation receives a weight that corresponds to the fraction of ancestors, many generations ago, that originated from this particular subpopulation. When subpopulations are weighted in this way, the overall frequency of an allele in the metapopulation changes over time in such a way that only genetic drift (term I) contributes, whereas the effects of migration into different subpopulations cancel out ($II = 0$). These so called reproductive subpopulation weights give rise to a version of the variance effective size that we refer to as N_{eVMeta}. It turns out that N_{eVMeta} is of particular interest for long term conservation, since under migration–drift equilibrium N_{eVMeta} not only equals N_{eGD} and N_{eAV}, but also the eigenvalue effective size N_{eE} (Ewens 1982, 2004), which is known to reflect the long term genetic behavior of a population.

In spite of the relevance of N_{eVMeta} for conservation, it is a challenge to use this effective size in practice since its subpopulation weights involve migration rates between subpopulations, which are difficult to estimate. It is possible, though, to find simplified expressions for I and II under migration–drift equilibrium, using perturbation theory and eigenvalue decomposition of matrices (Horn and Johnson 1985; Friswell 1996; Van der Aa et al. 2007). Although perturbation results for eigenvalues have previously been applied to population genetics (Maruyama 1970a; Nagylaki 1980, 1995; Hössjer 2015) it seems that our perturbation results for eigenvectors are new. Based on this analysis we demonstrate, for some particular models, that it is possible to eliminate the impact II of migration by maximizing the variance effective size with respect to subpopulation weights, so that the corresponding N_{eV} approximates N_{eVMeta}.

For the second contribution (ii) of this article, we demonstrate that when the impact II of gene flow is not eliminated, under certain conditions it elevates allele frequency change over long time intervals to such an extent that the traditional (forward) version of N_{eV} is undefined. For this reason we define two novel notions of variance effective size, the intermediate and backward versions of N_{eV}. The

intermediate version corresponds to a frequently used estimator of variance effective size due to Jorde and Ryman (2007), and although it is more stable than the forward version of N_{eV}, it shares the drawback of sometimes being undefined for long time intervals of genetic change. The backward version of N_{eV}, on the other hand, exists for most populations, and it is also the version of variance effective size that most closely relates to N_{eGD} and N_{eE}, since it lessens the impact of the gene flow term *II* more than the other two versions of variance effective size. We demonstrate, numerically and analytically, that the forward, intermediate and backward versions of the local variance effective size are very close for large subdivided populations, unless the time interval is very long. On the other hand, the three effective sizes differ substantially for a small and subdivided population, and moderate or large time intervals.

For the third contribution (iii) of this article, we give explicit expressions for the length of the time interval that maximizes the accuracy of estimates of N_{eGD} and all three versions of N_{eV}, for any type of subpopulation weights. This optimal length is proportional to the eigenvalue effective size N_{eE}, with a constant of proportionality that depends on characteristics of the population as well as the type of effective size being used, including subpopulation weights. This reinforces that the three variance effective sizes behave differently for small subdivided populations (when N_{eE} is small).

Our paper is organized as follows: We start by defining the population genetic model in Sect. 2, and the framework of genetic variation in terms of one single biallelic marker in Sect. 3. This makes it possible in Sect. 4 to introduce the matrix analytic framework for how covariances of allele frequency change, gene diversities and fixation indeces evolve over time. The various notions of effective size are introduced in Sect. 5, migration–drift equilibrium is the topic of Sect. 6, the impact of the length of the time interval on effective size is analyzed in Sect. 7, and the optimal time interval in terms of accurately estimating effective size is studied in Sect. 8. Then analysis of a real data set in Sect. 9 and a discussion in Sect. 10 concludes. A summary of the most important notation is provided in Table 1, whereas some of the numerical results and all proofs are collected in the appendices.

2 Population Genetic Model

We will study the genetic composition of a structured (or subdivided) population that evolves over time in terms of non-overlapping generations $t = -T, -T+1, \ldots$, where $-T \leq 0$ is a founder generation. The population has s subpopulations $x = 1, \ldots, s$, whose local census sizes N_{cx} and local effective sizes N_{ex} under isolation do not change over time. The subpopulations are not isolated, but rather connected though gene flow, as summarized by an irreducible backward migration matrix $\boldsymbol{B} = (B_{xy})$ of order s, where B_{xy} is the expected fraction of gene copies in x that in the previous generation migrated from y.

The most well known type of subdivided population is the island model (Wright 1943; Maruyama 1970b), for which $N_{ex} = N_e$ and $N_{cx} = N_c$ are the same for all subpopulations. The migration rates $B_{xy} = m'/(s-1) = m/s$ between all pairs $x \neq y$

Table 1 A summary of the most important notation used in this article

Quantity	Description
s	Number of subpopulations
x, y	Index of a subpopulation ($\in \{1, \dots, s\}$)
t	Time index, in units of generations ($\in \{-T, -T+1, \dots\}$)
T	Number of generations ago ($t = -T$) when the founder population lived
τ	Length of time interval along which genic change is assessed
B_{xy}	Backward migration rate from x to y or the fraction of parents of individuals in subpopulation x that originate from subpopulation y one generation ago
$\boldsymbol{B}$	Square matrix $(B_{xy})_{x,y=1}^{s}$ of order s with all backward migration rates
m'	Migration rate of island model ($B_{xy} = m'/(s-1)$ when $x \neq y$)
m	Fraction of parents in the island model that originate from the whole population one generation ago ($= sm'/(s-1)$)
w_x	Weight of subpopulation x at the start ($= t$) of the time interval along which genetic change is assessed
$\boldsymbol{w}$	Vector of subpopulation weights ($= (w_1, \dots, w_s)$) at the start of the time interval along which genetic change is assessed
v_x	Weight of subpopulation x at the end ($= t + \tau$) of the time interval along which genetic change is assessed
$\boldsymbol{v}$	Vector of subpopulation weights ($= (v_1, \dots, v_s)$) at the end of the time interval along which genetic change is assessed
$\boldsymbol{e}_x$	Vector of local subpopulation weights ($= (0, \dots, 0, 1, 0, \dots, 0)$) that only assigns a positive weight to subpopulation x (a 1 in position x)
$\boldsymbol{\gamma}$	Vector of reproductive subpopulation weights ($= (\gamma_1, \dots, \gamma_s)$). γ_x is the fraction of ancestors originating from subpopulation x many generations ago
A	One of the two alleles of a biallelic marker
p	Frequency of A in all subpopulations in the founder generation
p_{tx}	Frequency of allele A in subpopulation x and generation t
p_t	Weighted frequency of allele A in the whole population in generation t, when subpopulations are weighted as $\boldsymbol{w}$ ($= \sum_x w_x p_{tx}$)
$p_{t+\tau}$	Weighted frequency of allele A in the whole population in generation $t + \tau$, when subpopulations are weighted as $\boldsymbol{v}$ ($= \sum_x v_x p_{t+\tau,x}$)
$\mathbf{1}_n$	Column vector of length n with ones in all positions
h_{tx}	$1 - h_{tx}$ is the standardized covariance of allele frequency change from the base generation to generation t, between subpopulations x and y
$\boldsymbol{h}_t$	Column vector of length s^2 with all the one minus standardized covariances at time t ($= (h_{txy})_{x,y=1}^{s}$)
H_{txy}	Gene diversity between subpopulations x and y in generation t
$\boldsymbol{H}_t$	Column vector of length s^2 with all gene diversities at time t ($= (H_{txy})_{x,y=1}^{s}$)
$\boldsymbol{A}$	Square matrix of order s^2 describing a linear time recursion of $\boldsymbol{h}_t$ and $\boldsymbol{H}_t$
λ	Largest eigenvalue of $\boldsymbol{A}$
$\boldsymbol{r}$	Right eigenvector of $\boldsymbol{A}$ with eigenvalue λ
$F_{ST,t}$	Fixation index in generation t
F_{ST}^{eq}	Fixation index under migration–drift equilibrium
N_e	Generic notation for effective population size
N_{cx}	Local census size of subpopulation x ($= N_c$ if all N_{cx} are identical)
N_{ex}	Local effective size of an isolated subpopulation x ($= N_e$ if all N_{ex} are identical)

Table 1 (continued)

Quantity	Description
Q	Quantity used for defining type of effective population size
N_{eQ}	Generic notation for effective population size of type Q
N_{eQ}^{eq}	Generic notation for effective size of type Q at migration–drift equilibrium
$N_{eQ\boldsymbol{wv}}$	Effective population size when subpopulations are weighted as $\boldsymbol{w}$ and $\boldsymbol{v}$ at the two end points of the interval along which genetic change is assessed
$N_{eQ\boldsymbol{w}}$	Effective population size when subpopulations are weighted as $\boldsymbol{w}$ at both end points of the interval along which genetic change is assessed (= $N_{eQ\boldsymbol{ww}}$)
N_{eQMeta}	Effective size of type Q for the metapopulation (= $N_{eQ\boldsymbol{\gamma}} = N_{eQ\boldsymbol{\gamma\gamma}}$)
N_{eQRx}	Realized local effective size of type Q for subpopulation x (= $N_{eQ\boldsymbol{e}_x} = N_{eQ\boldsymbol{e}_x\boldsymbol{e}_x}$). It equals N_{ex} when x is isolated from the other subpopulations
N_{eQRxy}	Realized local effective size of type Q when subpopulations x and y ($x \neq y$) receive full weight at the two end points of the time interval (= $N_{eQ\boldsymbol{e}_x\boldsymbol{e}_y}$)
N_{eGD}	Generic notation for gene diversity effective size
N_{eAV}	Generic notation for additive genetic variance effective size
N_{eV}	Generic notation for forward version of variance effective size
N_{eV}^{int}	Generic notation for intermediate version of variance effective size
N_{eV}^{back}	Generic notation for backward version of variance effective size
N_{eE}	Eigenvalue effective size (it has only one version that describes long term change at migration–drift equilibrium and it does not involve subpopulation weights)
$I_{T+t}(\tau)$	Contribution to expected squared allele frequency change between generations t and $t+\tau$ from decreased gene diversity between these two generations. $I_{T+t}(\tau)$ is referred to as a genetic drift term (generic notation I, equals $I_\infty(\tau)$ at migration–drift equilibrium)
$II_{T+t}(\tau)$	$-II_{T+t}(\tau)$ is the contribution, to expected squared allele frequency change between generations t and $t+\tau$, from correlation between allele frequency change between these two generations and allele frequency of the past, before time t. $II_{T+t}(\tau)$ is mainly caused by migration and it is therefore often referred to as a migration or gene flow term (generic notation II, equals $II_\infty(\tau)$ at migration–drift equilibrium)

of subpopulations are the same as well, so that in each generation $m' = 1 - B_{xx}$ is the fraction of offspring of subpopulation x whose parents migrated from any other subpopulation $\{y; y \neq x\}$. On the other hand, m can be thought of as the fraction of offspring of x whose parents originate from a global gene pool, with equal contribution from all subpopulations (including x itself). The one- and two-dimensional stepping stone models (Kimura 1953; Kimura and Weiss 1964; Weiss and Kimura 1965; Durrett 2008) correspond to a subdivided population where migration from y to x ($B_{xy} > 0$) is possible only when these two subpopulations are neighbors.

It is assumed that the population reproduces in such a way that migration precedes fertilization. More specifically, reproduction between generations t and $t+1$ involves the following three steps:

1. (Gamete formation) Within each subpopulation x of generation t an infinitely large pre-migration gene pool is constructed as follows: $2N_{ex}$ gene copies (corresponding to N_{ex} diploid breeders) are drawn without replacement from all

$2N_{cx}$ gene copies (corresponding to N_{cx} diploid individuals) of this subpopulation x at time t. All $2N_{ex}$ drawn gene copies multiply and contribute in equal proportions $1/(2N_{ex})$ to the infinite pre-migration pool of x. These s pre-migration gene pools ($x = 1, \ldots, s$) are constructed independently for all subpopulations, without any exchange of genetic material.

2. (Migration) The s pre-migration gene pools of step 1 mix, so that s post-migration pools are formed. In particular, the post-migration pool of subpopulation x is a mixture of the pre-migration pools of subpopulations $1, \ldots, s$ in proportions $B_{x1}, \ldots, B_{xs}$.
3. (Fertilization) The $2N_{cx}$ gene copies (corresponding to N_{cx} diploid individuals) of subpopulation x and generation $t+1$ are formed by sampling $2N_{cx}$ genes from the post-migration gene pool of x. This is done independently between all subpopulations $x = 1, \ldots, s$.

We refer to this reproduction scenario as MF/FF, an acronym for migration preceding fertilization, with fixed migrant proportions and fixed migrant allele frequencies. It was used in Hössjer et al. (2013) for the island model and in Hössjer et al. (2014) and Olsson et al. (2017) for subdivided populations of general form. A number of other, closely related reproduction schemes were studied in the context of the island model by Hössjer et al. (2013) and more generally by Hössjer and Ryman (2014).

3 Genetic Variation at a Biallelic Marker

Our main focus is to study how the genetic composition of the population of Sect. 2 changes between two time points t and $t+\tau$, where τ is a positive integer. Typically genetic data from many biallelic markers are used to represent the genetic composition at time t and $t+\tau$. For our theoretical investigations in Sects. 3–8, it will be sufficient though to study one single biallelic marker, as a representative of any of the markers that are part of the data set. For this reason we consider a marker with alleles A and a and let p_t be the frequency of allele A in generation t. For a subdivided population we need to keep track of the frequency p_{tx} of A in all subpopulations x at each time point t. In order to obtain one single allele frequency at time t and $t+\tau$, we will weight subpopulations as $\boldsymbol{w} = (w_1, \ldots, w_s)$ and $\boldsymbol{v} = (v_1, \ldots, v_s)$ at these two time points, where w_x and v_x are non-negative numbers satisfying $\sum_x w_x = \sum_x v_x = 1$. The accompanying subpopulation weighted frequencies of A, at time t and $t+\tau$, are

$$\begin{aligned} p_t &= \textstyle\sum_x w_x p_{tx}, \\ p_{t+\tau} &= \textstyle\sum_x v_x p_{t+\tau,x}. \end{aligned} \tag{1}$$

The subpopulation weights in (1) play a crucial role in this paper. They may for instance reflect the sampling scheme of time points t and $t+\tau$, although this is not necessary. Local subpopulation weights at time t correspond to giving some subpopulation x full weight ($w_x = 1$), whereas none of the other subpopulation contribute to p_t ($w_y = 0$ for any $y \neq x$). With vector notation this is phrased as $\boldsymbol{w} = \boldsymbol{e}_x$, where $\boldsymbol{e}_x = (0, \ldots, 0, 1, 0, \ldots, 0)$ has a one in position x and zeros elsewhere.

Similarly, $v_x = 1$ if subpopulation weight x receives full weight at time $t + \tau$, or equivalently $\boldsymbol{v} = \boldsymbol{e}_x$. Global subpopulation weights at time t and $t + \tau$ assign positive values $w_x > 0$ and $v_x > 0$ respectively, to all subpopulations x. When the long term evolution of the population is of interest, it is appropriate to use reproductive subpopulation weights $\boldsymbol{w} = \boldsymbol{v} = \boldsymbol{\gamma} = (\gamma_1, \ldots, \gamma_s)$ at both time points, since a fraction γ_x of all gene copies originated from subpopulation x many generations ago (Nagylaki 1980, 2000; Hössjer and Ryman 2014). This weight vector $\boldsymbol{\gamma}$ is the equilibrium distribution of a Markov chain with state space $\{1, \ldots, s\}$ and transition matrix $\boldsymbol{B}$, and it corresponds to a probability distribution for the subpopulation ancestry of a gene copy. Assuming that $\boldsymbol{B}$ is irreducible, $\boldsymbol{\gamma}$ is the unique probability vector satisfying $\boldsymbol{\gamma} = \boldsymbol{\gamma B}$, with $\boldsymbol{\gamma} = (1, \ldots, 1)/s$ for the island model. Consequently, γ_x quantifies the long term contribution of x to the metapopulation, or as mentioned above, γ_x is the fraction of ancestors that originated from x, many generations back in time.

4 Standardized Covariances, Gene Diversities, and Fixation Indeces

In this section we define a number of concepts needed in Sect. 5 when various types of effective size are introduced. Following Hössjer et al. (2016), assume that all subpopulations have the same frequency $p_{-T,x} = p$ of allele A at the founder generation at $t = -T$. This is no essential restriction, since we will mainly consider equilibrium conditions when $T \to \infty$.

4.1 Standardized Covariances

The standardized covariance between a pair x, y of subpopulations at time point $t \in \{-T, -T + 1, \ldots\}$, is defined as

$$f_{txy} = \frac{\text{Cov}\,(p_{tx} - p, p_{ty} - p)}{p(1-p)} = 1 - h_{txy}. \tag{2}$$

Equivalently, f_{txy} is the correlation coefficient between the alleles of two gene copies drawn independently from subpopulations x and y at time t (with replacement if $x = y$), see for instance Cockerham (1969). It was shown in Hössjer et al. (2014) that the column vector $\boldsymbol{h}_t = (h_{txy})$ of length s^2 satisfies a recursive relation

$$\boldsymbol{h}_{t+1} = \boldsymbol{A}\boldsymbol{h}_t, \tag{3}$$

where $\boldsymbol{A} = (A_{xy,zu})$ is a square matrix of order s^2 with elements

$$A_{xy,zu} = \left(1 - \frac{1}{2N_{cx}}\right)^{1(x=y)} B_{xz} B_{yu} \left(\frac{1 - \frac{1}{2N_{ez}}}{1 - \frac{1}{2N_{cz}}}\right)^{1(z=u)}. \tag{4}$$

Similar types of recursions were originally developed by Malécot (1951), see also Whitlock and Barton (1997). Since all standardized covariances vanish at the founder generation, it follows that

$$\boldsymbol{h}_{-T} = \mathbf{1}_{s^2} = (1, \ldots, 1)^T \tag{5}$$

is a vector of s^2 ones. Notice that the initial condition (5) and the linear recursion (3) determine the value of h_{txy} for all t, x, y.

4.2 Gene Diversities

The gene identity (gene diversity) F_{txy} (H_{txy}) between a pair of subpopulations at time t is the probability that two randomly chosen gene copies of subpopulations x and y, drawn with replacement if $x = y$, have the same (different) alleles. It turns out that the time recursive behavior of gene diversities is very similar to that of standardized covariances. In order to motivate this we notice that allele frequencies at time $t > -T$ are unknown from the perspective of the base generation $-T$, and therefore

$$H_{txy} = E\big[p_{tx}(1 - p_{ty}) + (1 - p_{tx})p_{ty}\big].$$

This implies that the gene diversities at time t and $t + \tau$ are given by

$$\begin{aligned} H_t &= E\big[2p_t(1 - p_t)\big] = \textstyle\sum_{x,y} w_x w_y H_{txy}, \\ H_{t+\tau} &= E\big[2p_{t+\tau}(1 - p_{t+\tau})\big] = \textstyle\sum_{x,y} v_x v_y H_{t+\tau,xy}. \end{aligned} \tag{6}$$

By this we mean that H_t is the probability that two gene copies, drawn randomly with replacement from the population at time t, have different alleles, given that w_x is the probability of drawing each gene from x. Likewise, $H_{t+\tau}$ is the probability that two randomly drawn gene copies at time $t + \tau$ have different alleles, if subpopulations are chosen with probabilities v_x. It was shown in Hössjer et al. (2014) that the column vector $\boldsymbol{H}_t = (H_{txy})$ of length s^2 satisfies the same recursion as in (3), i.e.

$$\boldsymbol{H}_{t+1} = \boldsymbol{A}\boldsymbol{H}_t, \tag{7}$$

for $t = -T, -T + 1, \ldots$. Since $p_{-T,x} = p$ by assumption, we have that $H_{-Txy} = 2p(1 - p)$ for all x, y, and consequently

$$\boldsymbol{H}_{-T} = 2p(1 - p)\mathbf{1}_{s^2}. \tag{8}$$

Comparing (3) and (5) with (7) and (8), we find that the numbers h_{txy} obtained from the standardized covariances are equivalent to the gene diversities H_{txy}, up to a multiplicative constant, i.e.

$$H_{txy} = 2p(1 - p)h_{txy} \tag{9}$$

for all t, x, y.

A concept closely related to (6) is the collection of gene diversities *without replacement*. They are defined as

$$\begin{aligned} \tilde{H}_t &= \sum_{x,y} w_x w_y \tilde{H}_{txy}, \\ \tilde{H}_{t+\tau} &= \sum_{x,y} v_x v_y \tilde{H}_{t+\tau,xy}, \end{aligned} \tag{10}$$

the probabilities that two gene copies, drawn randomly *without* replacement at the same time point t and $t+\tau$ respectively, have different alleles. Likewise, $\tilde{H}_{txy}$ is the probability that two gene copies, drawn at randomly without replacement from x and y at time t, have different alleles. It was shown in Hössjer et al. (2014) that the column vector $\tilde{\boldsymbol{H}}_t = (\tilde{H}_{txy})$ of gene diversities without replacement satisfies a recursion

$$\tilde{\boldsymbol{H}}_{t+1} = \boldsymbol{D}\tilde{\boldsymbol{H}}_t \tag{11}$$

for $t = -T, -T+1, \ldots$, where $\boldsymbol{D} = (D_{xy,zu})$ is a square matrix of order s^2 with elements

$$D_{xy,zu} = B_{xz}B_{yu}\left(1 - \frac{1}{2N_{ez}}\right)^{1(z=u)}. \tag{12}$$

Note that the definitions of $\tilde{H}_{txy}$ and H_{txy} are the same when $x \neq y$. Moreover, since $(2N_{cx}-1)/(2N_{cx})$ is the probability that two gene copies, drawn randomly with replacement from x, are different copies, it follows that

$$\tilde{H}_{txy} = H_{txy}\left(\frac{2N_{cx}}{2N_{cx}-1}\right)^{I(x=y)} \tag{13}$$

for all x, y. In particular, a comparison between (8) and (13) reveals that $\tilde{\boldsymbol{H}}_{-T}$ is virtually independent of the census sizes N_{cx} when these are large. Since the elements (12) of the linear recursion matrix $\boldsymbol{D}$ do not involve any census sizes, it follows that $\tilde{H}_{txy}$ are virtually independent of census sizes as well, for any t, x, y. Making use of (13) again, we conclude that the gene diversities H_{txy} are virtually independent of the local census sizes as well.

4.3 Fixation Index

The most well known measure of genetic differences between subpopulations is the fixation index F_{ST} (Malécot 1948, Wright 1949; Weir and Cockerham 1984; Bhatia et al. 2013). Here we will use a version of the fixation index referred to as the coefficient of gene differentiation by Nei (1973) and subsequently generalized to multiallelic loci in Nei (1977). The fixation index is conveniently defined in terms of allele frequency differences between subpopulations, and we will study F_{ST} in each generation t from the perspective of the base generation $-T$, so that allele frequencies at $t > -T$ are unknown. Following the argument in Hössjer et al. (2016), the fixation index at time t is then predicted by

$$F_{ST,t} = \frac{\sum_{x=1}^{s} w_x E\left[(p_{tx} - p_t)^2\right]}{E[p_t(1-p_t)]} = \frac{\sum_{x,y} w_x w_y h_{txy} - \sum_x w_x h_{txx}}{\sum_{x,y} w_x w_y h_{txy}}, \tag{14}$$

where in the last step of (14) we first divided the numerator and denominator by $p(1-p)$, and then invoked the definition of $h_{txy} = 1 - f_{txy}$ in (2). In order for the fixation index to be nonzero, it is required that at least two subpopulation weights w_x are nonzero. We will mainly use (14) in the context of reproductive population weights $\boldsymbol{w} = \boldsymbol{\gamma}$.

5 Effective Sizes

The idea of effective size is to find a simple population that serves as a yardstick and shares some properties with the structured population of interest. The Wright–Fisher population (WF) is usually used for this purpose. It is a special case of the model of Sect. 2 that corresponds to a homogeneous population ($s = 1$) with equal census and effective size ($N_{c1} = N_{e1} = N$). An effective size of type Q (notated as N_{eQ}) is the size of a WF population that exhibits the same value of a certain quantity Q as the given structured population. Typically Q quantifies how fast the genetic composition of the population changes between time points t and $t + \tau$, and we will assume that it takes the value $(1 - 1/(2N))^\tau$ for a WF population of size N, so that

$$Q = Q(\tau) = 1 - \left(1 - \frac{1}{2N_{eQ}}\right)^\tau. \tag{15}$$

Solving for the effective size in (15) we find that

$$N_{eQ} = \frac{1}{2\{1 - [1 - Q(\tau)]^{1/\tau}\}}. \tag{16}$$

Equation (16) is very close to a formula for the effective size that appears at the bottom of Page 525 of Luikart et al. (1999). Since they have $2N_{eQ} + 1$ rather than $2N_{eQ}$ in the denominator of (15), they end up with an additional term -0.5 in the expression for N_{eQ}, and they also include extra terms that correct for estimation bias of $Q(\tau)$ due to having finite samples of genetic data at time points t and $t + \tau$.

When $N_{eQ} \gg \tau$, the right hand side of (15) is well approximated by a first order Taylor expansion of $g(x) = 1 - (1-x)^\tau \approx \tau x$ around $x = 0$. This gives rise to the simpler and approximate definition

$$N_{eQ,\text{add}} = \frac{\tau}{2Q(\tau)}. \tag{17}$$

Sometimes (17) is referred to as the additive approach (Waples 1989; Luikart et al. 1999), as opposed to the exact multiplicative approach (15). Although the additive approximation often works well, it can sometimes be inaccurate when τ gets large, in particular for populations that experience bottlenecks (Richards and Leberg 1996;

Luikart et al. 1999). Another important difference between the multiplicative and additive approaches is that $N_{eQ,\mathrm{add}}$ always exists, as long as Q is positive, whereas in order for N_{eQ} to have a finite positive value we must require $0 < Q < 1$. Although $Q < 1$ is guaranteed for a Wright–Fisher population, for a subdivided population in general Q may sometimes exceed in 1.

In this paper we will mainly focus on loss of gene diversity ($Q = GD$) and variance of allele frequency change ($Q = V$). But we will also consider the eigenvalue effective size, for which $Q = E$ corresponds to the largest eigenvalue of a certain matrix. This effective size does not follow the general pattern (15) and (16) of genetic change between two time points t and $t + \tau$, but rather it quantifies the long term loss of genetic diversity at migration–drift equilibrium.

5.1 Notation for Local and Global Effective Sizes

We will assume that subpopulations are weighted as $\boldsymbol{w}$ and $\boldsymbol{v}$ at time t and $t + \tau$, and in order to highlight the impact of these subpopulation weights we sometimes write $N_{eQ} = N_{eQ\boldsymbol{wv}}$, and in particular $N_{eQ} = N_{eQ\boldsymbol{w}}$ when the same weight vector $\boldsymbol{w} = \boldsymbol{v}$ is used at both time points. For an effective size of type $Q \in \{GD, V\}$ we also adopt the notation of Laikre et al. (2016) and write $N_{eQMeta} = N_{eQ\boldsymbol{\gamma}}$ for the effective population size of the metapopulation. This corresponds to using reproductive weights at both time points ($\boldsymbol{w} = \boldsymbol{v} = \boldsymbol{\gamma}$). The quantity $N_{eQRx} = N_{eQ\boldsymbol{e}_x}$ refers to the realized local effective size of subpopulation x, and it corresponds to using the same local weight vector at both time points ($\boldsymbol{w} = \boldsymbol{v} = \boldsymbol{e}_x$). The term realized was introduced in Laikre et al. (2016) and Ryman et al. (2019) to emphasize the fact that due to migration N_{eQRx} typically differs from N_{ex}, although the two quantities are identical when x is isolated from the other subpopulations. When two different subpopulations x and y receive full weight at time points t and $t + \tau$, i.e. $\boldsymbol{w} = \boldsymbol{e}_x$, $\boldsymbol{v} = \boldsymbol{e}_y$, and $x \neq y$, we write $N_{eQRxy} = N_{eQ\boldsymbol{e}_x\boldsymbol{e}_y}$ for the corresponding realized effective size.

The eigenvalue effective size N_{eE}, on the other hand, is a property of the metapopulation, and therefore it does not involve subpopulation weights.

5.2 Gene Diversity Effective Size

The gene diversity effective size N_{eGD} between the two time points t and $t + \tau$ is defined as the size of an ideal Wright–Fisher population that exhibits the same relative gene diversity decline (locally or globally for the metapopulation), during this time interval, as for the studied structured population. In mathematical terms, this corresponds to the quantity

$$Q(\tau) = 1 - \left(1 - \frac{1}{2N_{eGD}}\right)^{\tau} = \frac{H_t - H_{t+\tau}}{H_t} =: I, \tag{18}$$

where $I = I_{T+t}(\tau)$, the relative decline of gene diversity, quantifies how much genetic drift there has been between generations t and $t + \tau$.

The effective size in (18) was referred as a haploid inbreeding effective size with replacement in Hössjer et al. (2014), since gene diversity decrease is equivalent to gene identity increase, a haploid analogue of increased inbreeding. It was shown in Hössjer et al. (2016) that N_{eGD} is a good approximation of the additive genetic variance effective size N_{eAV}, which is of interest for long term conservation of species. Recall from the discussion at the end of Sect. 4.2 that all H_{txy} and $H_{t+\tau,xy}$ are essentially independent of the local census sizes of all subpopulations. From this it follows that H_t, $H_{t+\tau}$, I, and N_{eGD} are functions of the migration rates in $\boldsymbol{B}$ and the local effective sizes N_{ex}, whereas they are essentially independent of the local census sizes N_{cx}. Since I is nonzero even when all subpopulations are isolated, the contribution of all N_{ex} is most fundamental to I, and for this reason we will refer to it as a genetic drift term.

Since the gene diversities H_t and $H_{t+\tau}$ are non-negative, it follows that the term I does not exceed unity ($I \leq 1$). It may happen though that I is negative when local subpopulations weights of x are used at both time points ($\boldsymbol{w} = \boldsymbol{v} = \boldsymbol{e}_x$) and migration into x causes the gene diversity to increase ($H_{t+\tau} > H_t$). Then formally $N_{eGD} = \infty$.

5.3 Variance Effective Size

5.3.1 Forward Approach

The variance effective size N_{eV} is the size of an ideal and spatially homogeneous population whose standardized variance of allele frequency change between time points t and $t + \tau$ is the same as in the studied structured population, see for instance Sect. 7.6.3 of Crow and Kimura (1970). It is instructive to first introduce N_{eV} for a population that is either spatially homogeneous ($s = 1$) or has a substructure that is ignored. The traditional definition

$$1 - \left(1 - \frac{1}{2N_{eV}^{\text{trad}}}\right)^{\tau} = \frac{\text{Var}\,(p_{t+\tau} - p_t|p_t)}{p_t(1-p_t)} = F_{\text{trad}} \tag{19}$$

quantifies variance of allele frequency change conditionally on allele frequencies of generation t. If mutations and selection of a homogeneous population is ignored, then typically allele frequency change of the past (before time t) is uncorrelated with allele frequency change of the present (between time points t and $t + \tau$). This implies that $E(p_{t+\tau}|p_t) = p_t$, so that the variance in (19) equals $E[(p_{t+\tau} - p_t)^2|p_t]$. It turns out that the latter quantity is preferable to use in more general settings (such as a subdivided population) when possibly $E(p_{t+\tau}|p_t) \neq p_t$, due to the fact that allele frequency change of the past might be correlated with allele frequency change between time points t and $t + \tau$. We therefore define the variance effective size of a subdivided population (with subpopulation weights $\boldsymbol{w}$ and $\boldsymbol{v}$) as

$$Q(\tau) = 1 - \left(1 - \frac{1}{2N_{eV}}\right)^{\tau} = \frac{E[(p_{t+\tau} - p_t)^2]}{E[p_t(1-p_t)]} = F. \tag{20}$$

Equation (20) differs from (19) in that the numerator and denominator of the genetic drift term F are averaged with respect to p_t. Indeed, it is well known (Ewens 1982; Hössjer and Ryman 2014; Hössjer et al. 2014, 2016) that typically $E[(p_{t+\tau}-p_t)^2|p_t]/[p_t(1-p_t)]$ is not a fixed number for a structured population, but rather a function of p_t. This makes the more general definition of genetic drift in (20) preferable for a metapopulation with subpopulations, since the impact of p_t is averaged out. We will refer to (20) as the *forward* definition of N_{eV}, since allele frequency change is normalized, in the denominator, as a function of allele frequencies at time t, the left end point of the interval $[t, t+\tau]$, and from the perspective of this time point the allele frequency change in the numerator of (20) takes place forwards in time. Note that the traditional definition (19) of variance effective size is based on the forward approach as well, and it can be seen that (20) is a generalization of (19). In particular, when $\tau = 1$ and the population is homogeneous, both of (19) and (20) reduce to the well know formula $N_{eV} = p_t(1-p_t)/[2\ \mathrm{Var}\ (p_{t+1}-p_t|p_t)]$, see for instance Crow and Kimura (1970, Eq. 7.6.3.25).

Following Hössjer et al. (2016), where the special case $\boldsymbol{w} = \boldsymbol{v}$ was treated, we rewrite the right hand side of (20) as

$$\begin{aligned} 1-\left(1-\frac{1}{2N_{eV}}\right)^{\tau} &= \frac{E[(p_{t+\tau}-p_t)^2]}{E[p_t(1-p_t)]} \\ &= \frac{E[(p_{t+\tau}-p)^2]-E[(p_t-p)^2]}{E[p_t(1-p_t)]} + \frac{-2\mathrm{Cov}(p_{t+\tau}-p_t, p_t-p)}{E[p_t(1-p_t)]} \\ &= \frac{E[(p_{t+\tau}-p)^2]/[p(1-p)]-E[(p_t-p)^2]/[p(1-p)]}{E[p_t(1-p_t)]/[p(1-p)]} \\ &\quad + \frac{-2\mathrm{Cov}(p_{t+\tau}-p_t, p_t-p)/[p(1-p)]}{E[p_t(1-p_t)]/[p(1-p)]} \\ &= I + II. \end{aligned} \tag{21}$$

The first term I on the right hand side of (21) is identical to the genetic drift term I that appears in the definition (18) of the gene diversity effective size. Indeed, it follows from (2) and (21) that

$$I = I_{T+t}(\tau) = \frac{\sum_{x,y} w_x w_y h_{txy} - \sum_{x,y} v_x v_y h_{t+\tau,xy}}{\sum_{x,y} w_x w_y h_{txy}} \tag{22}$$

can be expressed in terms of h_{txy} and $h_{t+\tau,xy}$ for all pairs x, y of subpopulations, which in view of (9) are proportional to the corresponding gene diversities that appear in the genetic drift term I of (18).

The second term II of (21) is only present in a subdivided population, and therefore it follows from (18) and (21) that $N_{GD} = N_{eV}$ for homogeneous populations. For a subdivided population, $-II$ accounts for the correlation between allele frequency change up to time t, and the allele frequency change that takes place between time points t and $t+\tau$. We could therefore refer to $-II$ as a correlation between past and present allele frequency change. Extending the argument in Hössjer et al. (2016), where the case $\boldsymbol{w} = \boldsymbol{v}$ was treated, one finds that

$$II = II_{T+t}(\tau) = \frac{2\sum_{x,y}((\boldsymbol{v}\boldsymbol{B}^{\tau})_x - w_x) w_y h_{txy}}{\sum_{x,y} w_x w_y h_{txy}}. \tag{23}$$

It follows from (23) that $II = 0$ when all subpopulations are isolated ($\boldsymbol{vB} = \boldsymbol{v}$) and the subpopulation weights are the same at time points t and $t + \tau$ ($\boldsymbol{w} = \boldsymbol{v}$). We will therefore often refer to II as a migration or gene flow term, since it is impacted by migration in an essential way.

Equation (20) implies that the standardized amount of allele frequency change is non-negative, i.e. $F = I + II \geq 0$. It turns out that the gene flow term II is typically non-negative as well, since migration tends to induce a negative correlation between past and present allele frequency change when subpopulations with large allele frequencies receive inflow from other subpopulations with lower frequencies of the same allele. The consequence of such a negative correlation, or positive II, is to inflate the expected squared allele frequency change F. Since past and present allele frequency changes of a homogeneous population ($s = 1$) are uncorrelated, such a population must have $II = 0$ and $N_{eV} = N_{eGD}$. The same is true when subpopulations are weighted according to their long term reproductive ability ($\boldsymbol{w} = \boldsymbol{v} = \boldsymbol{\gamma}$), since positive and negative allele frequency changes in different subpopulations will then cancel out in such a way that allele frequency change before time t is uncorrelated to the one that takes place over the interval $[t, t + \tau]$. On the other hand, II is typically positive when one subpopulation x receives full weight ($\boldsymbol{w} = \boldsymbol{v} = \boldsymbol{e}_x$), and this will lower N_{eVRx} below N_{eGD}. The magnitude of II for local subpopulation weights depends on the amount of subpopulation differentiation at time t (as quantified by $F_{ST,t}$) and the amount of gene flow between the subpopulations. It follows from (14) that this amount of subpopulation differentiation is reflected in terms of how much larger h_{txy} for pairs of different subpopulations $x \neq y$ are compared to all h_{txx}. In the extreme case when all elements of $\boldsymbol{h}_t$ are the same it follows that $F_{ST,t} = II = 0$ and consequently $N_{eV} = N_{eGD}$. This happens for instance when the first time point t of $[t, t + \tau]$ is the founder generation ($t = -T$). On the other hand, when $II > 0$ it may happen that $F = 1 \Leftrightarrow II = 1 - I$ or $F > 1 \Leftrightarrow II > 1 - I$, which we formally write as $N_{eV} = 0$ and $N_{eV} = -\infty$ respectively.

5.3.2 Intermediate Approach

The forward definition (20) of the variance effective size relies on a standardized measure $F = I + II$ of expected squared allele frequency change, which sometimes exceeds 1. This is due to the fact that the denominator of F in (20) is inflated when the allele frequency at the first time point t of the interval $[t, t + \tau]$ is close to 0 or 1. For this reason, when N_{eV} is estimated from data by the temporal method, allele frequency change is usually standardized in such a way that allele frequencies at both time points t and $t + \tau$ are used. In particular, the approach of Pollack (1983) and Jorde and Ryman (2007) corresponds to a definition

$$F^{\text{int}} = \frac{E[(p_{t+\tau} - p_t)^2]}{E[(p_t + p_{t+\tau})/2 \cdot (1 - (p_t + p_{t+\tau})/2)]} \tag{24}$$

of standardized expected squared allele frequency change, whose denominator involves allele frequencies p_t and $p_{t+\tau}$ at both time points t and $t+\tau$. We refer to (24) as the intermediate version of the standardized expected squared allele frequency change, since the allele frequency change of the numerator is forward *or* backward in time, from the perspective of time point t and $t+\tau$ respectively. Let N_{eV}^{int} refer to the corresponding intermediate version of variance effective size that makes use of F^{int} rather than F. It is not possible to define N_{eV}^{int} by simply replacing F with F^{int} in (20), since for a Wright–Fisher population, such a procedure would not retain the population size. Instead, following Jorde and Ryman (2007) we put

$$Q(\tau) = 1 - \left(1 - \frac{1}{2N_{eV}^{\text{int}}}\right)^{\tau} = \frac{F^{\text{int}}}{1 + \frac{1}{4}F^{\text{int}}}. \tag{25}$$

It can be seen that the intermediate approach is somewhat more stable than the forward approach. Indeed, the right hand side of (25) is less than 1 whenever $F^{\text{int}} < 4/3$, so that N_{eV}^{int} exists whenever $0 < F^{\text{int}} < 4/3$.

In order to analyze N_{eV}^{int} more closely, we need an expression for the genetic drift term F^{int} in (24). To this end, we have to replace the denominator $E[p_t(1-p_t)]$ of F in (20) by $E[(p_t + p_{t+\tau})/2 \cdot (1 - (p_t + p_{t+\tau})/2)]$. The ratio of these two denominators is

$$\begin{aligned}
\frac{E\left[\frac{p_t+p_{t+\tau}}{2}\left(1-\frac{p_t+p_{t+\tau}}{2}\right)\right]}{E[p_t(1-p_t)]} &= \frac{p(1-p)}{E[p_t(1-p_t)]} - \frac{E\left(\frac{p_t+p_{t+\tau}}{2}-p\right)^2}{E[p_t(1-p_t)]} \\
&= \frac{p(1-p)}{E[p_t(1-p_t)]} - \frac{3}{4}\frac{E[(p_t-p)^2]}{E[p_t(1-p_t)]} \\
&\quad - \frac{1}{4}\frac{E[(p_{t+\tau}-p)^2]}{E[p_t(1-p_t)]} - \frac{1}{2}\frac{\mathrm{Cov}(p_{t+\tau}-p_t, p_t-p)}{E[p_t(1-p_t)]} \\
&= 1 + \frac{1}{4}\frac{E[(p_t-p)^2]}{E[p_t(1-p_t)]} - \frac{1}{4}\frac{E[(p_{t+\tau}-p)^2]}{E[p_t(1-p_t)]} \\
&\quad - \frac{1}{2}\frac{\mathrm{Cov}(p_{t+\tau}-p_t, p_t-p)}{E[p_t(1-p_t)]} \\
&= 1 - \frac{1}{4}I + \frac{1}{4}II.
\end{aligned} \tag{26}$$

Inserting (21) and (26) into (24) we find that

$$F^{\text{int}} = \frac{I + II}{1 - \frac{1}{4}I + \frac{1}{4}II}. \tag{27}$$

When the last equation is plugged into (25), an expression

$$1-\left(1-\frac{1}{2N_{eV}^{\text{int}}}\right)^{\tau}=\frac{I+II}{1+\frac{1}{2}II} \tag{28}$$

is obtained for the intermediate definition of the variance effective size. From this it follows that the threshold for the intermediate version of the variance effective size not to exist ($N_{eV}^{\text{int}}=-\infty$) is twice as high ($II>2(1-I)$) as compared to the forward version of this effective size.

5.3.3 Backward Approach

In analogy with (24) and (25), we also introduce a novel *backward* definition of N_{eV}. In the first step expected squared allele frequency change

$$F^{\text{back}}=\frac{E[(p_{t+\tau}-p_t)^2]}{E[p_{t+\tau}(1-p_{t+\tau})]} \tag{29}$$

is normalized using allele frequencies from the right end point $t+\tau$ of the time interval along which genetic change is monitored. From the horizon of an observer at this time point (29) describes what happened in the past, since the expected squared allele frequency change of the numerator is applied to a time period of the past. Let N_{eV}^{back} denote the variance effective size that makes use of F^{back} rather than F. In order for N_{eV}^{back} to retain the size of a Wright–Fisher population, we need to define it as

$$Q(\tau)=1-\left(1-\frac{1}{2N_{eV}^{\text{back}}}\right)^{\tau}=\frac{F^{\text{back}}}{1+F^{\text{back}}}. \tag{30}$$

It follows that N_{eV}^{back} exists for all scenarios such that the standardized expected squared allele frequency change between generations t and $t+\tau$ satisfies $0<F^{\text{back}}<\infty$, since this implies $0<Q(\tau)<1$. For this reason the backward approach (30) gives a more stable definition of variance effective size than the forward and intermediate definitions in (20) and (25).

In order to study N_{eV}^{back} more closely, we start by deriving an expression for F^{back} in (29). To this end, we have to replace the denominator $E[p_t(1-p_t)]$ of F in (20) by $E[p_{t+\tau}(1-p_{t+\tau})]$. By similar calculations as in (26), we find that the ratio of these two denominators is

$$\frac{E[p_{t+\tau}(1-p_{t+\tau})]}{E[p_t(1-p_t)]}=1-I. \tag{31}$$

In a two-step procedure, we first insert (21) and (31) into (29) and find that

$$F^{\text{back}}=\frac{I+II}{1-I}. \tag{32}$$

When the last equation is plugged into (30), a formula

$$1 - \left(1 - \frac{1}{2N_{eV}^{\text{back}}}\right)^{\tau} = \frac{I + II}{1 + II} \tag{33}$$

for the backward definition of the variance effective size is derived. It follows that N_{eV}^{back} exists under the very mild requirements $I + II > 0$ and $I < 1$, since this implies $0 < Q(\tau) < 1$.

5.4 Eigenvalue Effective Size

The eigenvalue effective size N_{eE} corresponds to the long term rate at which genetic variability is lost. The formal definition of the eigenvalue effective size is

$$Q = \lambda = 1 - \frac{1}{2N_{eE}}, \tag{34}$$

where $\lambda = \lambda_3(\boldsymbol{P})$ is the largest non-unit eigenvalue and the third largest eigenvalue overall of the transition matrix $\boldsymbol{P}$ of $\{\boldsymbol{p}_t = (p_{t1}, \ldots, p_{ts}); t = -T, -T+1, \ldots\}$, the vector-valued Markov chain of allele frequencies in all subpopulations. This Markov chain is defined on a huge state space of size $\prod_{x=1}^{s}(2N_{cx}+1)$. Tufto et al. (1996) and Tufto and Hindar (2003) used a slightly different definition of λ in (34), as the largest eigenvalue

$$\lambda = \lambda_{\max}(\boldsymbol{A}) \tag{35}$$

of the much smaller matrix $\boldsymbol{A}$ that appears in the linear recursion for one minus standardized covariances as well as for gene diversities (cf. (3) and (7)). Indeed, by the Perron–Frobenius Theorem $\boldsymbol{A}$ has a unique, real-valued, and positive eigenvalue of multiplicity 1, which is strictly larger than the modulus of all other eigenvalues of $\boldsymbol{A}$. It follows from work of Whitlock and Barton (1997) and Hössjer (2015) that $\lambda_3(\boldsymbol{P}) = \lambda_{\max}(\boldsymbol{A})$.

5.5 Relations Between Effective Sizes

It is clear from the definition (18) of the gene diversity effective size and the three versions (21), (28), and (33) of the variance effective size that whenever the gene flow term II is non-negative ($II \geq 0$) the values of $Q(\tau)$ for these four effective sizes satisfy

$$I \leq \frac{I + II}{1 + II} \leq \frac{I + II}{I + \frac{1}{2}II} \leq I + II,$$

making use of the fact that $I \leq 1$ because of (18), and that $I + II \geq 0$ must hold as a consequence of (21). But since N_{eQ} is a strictly decreasing function of $Q(\tau)$ in (16), it follows that

$$N_{eV} \le N_{eV}^{\text{int}} \le N_{eV}^{\text{back}} \le N_{eGD}. \tag{36}$$

These inequalities involve the possibility that some effective sizes have values $-\infty$, 0, or ∞, whenever $Q(\tau) > 1$, $Q(\tau) = 1$ and $Q(\tau) \le 0$, as discussed above. There is no general relation between N_{eE} and the four effective sizes in (36). We will find however that under migration–drift equilibrium N_{eE} equals N_{eGD} as well as N_{eV} with reproductive subpopulation weights.

6 Migration–Drift Equilibrium

Migration–drift equilibrium occurs when many generations have elapsed between the founder generation and the first generation t of the interval over which genetic change is assessed, so that a balance between genetic drift within and migration between subpopulation is obtained. Mathematically, this corresponds to keeping t fixed while $T \to \infty$. Recall from (35) that $\boldsymbol{A}$ has a unique, real-valued, and largest eigenvalue λ. Let $\boldsymbol{r} = (r_{xy})$ be the corresponding right eigenvector of $\boldsymbol{A}$ with eigenvalue λ, whose elements, by the Perron–Frobenius Theorem, are real-valued and positive. In view of (5), it follows that $\boldsymbol{h}_{-T} = \mathbf{1}_{s^2} = C\boldsymbol{r} + \boldsymbol{r}'$ for some constant $C > 0$, where $\boldsymbol{r}'$ is a linear combination of the other right eigenvectors of $\boldsymbol{A}$. Consequently, it follows from the linear recursion (3) that

$$\boldsymbol{h}_t \approx C\lambda^{t+T}\boldsymbol{r} \tag{37}$$

is an increasingly accurate approximation as T gets large. For this reason the migration–drift properties of the metapopulation will only involve λ and $\boldsymbol{r}$.

Example 1 (Symmetric migration and equally large subpopulations) In order to find more explicit expressions for $\boldsymbol{r}$, we will consider a class of structured populations that includes the island and stepping stone models as special cases. These populations have subpopulations with equally large local census sizes ($N_{cx} = N_c$) and equally large local effective sizes under isolation ($N_{ex} = N_e$). The backward migration rates B_{xy} may depend on the pair x, y of subpopulations, but it is assumed that they are the same in both directions between any such pair. Consequently, the backward migration matrix $\boldsymbol{B}$ is symmetric ($B_{xy} = B_{yx}$ for all $x \ne y$). Since we also assume that $\boldsymbol{B}$ is irreducible, this implies that an asymptotic distribution $\boldsymbol{\gamma} = \mathbf{1}_s^T/s$ exists for the Markov chain with transition matrix $\boldsymbol{B}$, where $\mathbf{1}_s = (1, \dots, 1)^T$ is a column vector of s ones. Moreover, $\boldsymbol{B}$ has real-valued eigenvalues η_i, with

$$1 = \eta_1 > \eta_2 \ge \dots \ge \eta_s > -1.$$

Let $\boldsymbol{l}_1 = \sqrt{s}\boldsymbol{\gamma} = \mathbf{1}_s^T/\sqrt{s}, \boldsymbol{l}_2, \dots, \boldsymbol{l}_s$ be the corresponding orthonormal system of left eigenvectors $\boldsymbol{l}_i$ of $\boldsymbol{B}$, expressed as $\boldsymbol{l}_i = (l_{ix}; x = 1, \dots, s)$. It is shown in Appendix B.1 that the column vectors $\boldsymbol{l}_{ij}^T = (l_{ix}l_{jy}; 1 \le x, y \le s)^T$ of length s^2 form a convenient orthonormal system of basis functions to use in order to analyze the right eigenvector $\boldsymbol{r}$ of $\boldsymbol{A}$, for a system with symmetric migration.

The island model is an instance of symmetric migration, with

$$\boldsymbol{B} = (1-m)\boldsymbol{I}_s + m\mathbf{1}_s\mathbf{1}_s^T, \tag{38}$$

and $\boldsymbol{I}_s$ the identity matrix of order s. The non-unit eigenvalues of this migration matrix are

$$\eta_2 = \ldots = \eta_s = 1-m. \tag{39}$$

The circular stepping stone model is a second example of symmetric migration, where any subpopulation x receives a fraction $m/2$ of genes from each of its two neighboring subpopulations $x-1$ and $x+1$ modulo s. This corresponds to a backward migration matrix

$$\boldsymbol{B} = \begin{pmatrix} 1-m & m/2 & 0 & \ldots & m/2 \\ m/2 & 1-m & m/2 & \ldots & 0 \\ \vdots & & & \ddots & \vdots \\ m/2 & 0 & \ldots & m/2 & 1-m \end{pmatrix}. \tag{40}$$

The matrix in (40) is a circular matrix, and Fourier analysis of such matrices has frequently been used in population genetics (Malécot 1951; Maruyama 1970a; Rousset 2004; Hössjer 2014). For instance, it is shown in Hössjer (2014) that

$$\eta_i = 1 - m + m\cos\left(\frac{2\pi[(i+1)/2]}{s}\right), \quad i = 1, \ldots, s, \tag{41}$$

with $[(i+1)/2]$ the integer part of $(i+1)/2$. Expressions for η_i for the two-dimensional (torus) stepping stone model can be found in Hössjer (2014). □

6.1 Subpopulation Differentiation

In order to find an expression for the fixation index $F_{ST,t}$ under migration–drift equilibrium, we insert (37) into (14) and let $T \to \infty$. This yields

$$F_{ST,t} \xrightarrow{T\to\infty} F_{ST}^{\text{eq}} = \frac{\sum_{x,y} w_x w_y r_{xy} - \sum_x w_x r_{xx}}{\sum_{x,y} w_x w_y r_{xy}}, \tag{42}$$

where superscript eq is an acronym for equilibrium. It is shown in Appendix B.2 that for reproductive weights $\boldsymbol{w} = \boldsymbol{\gamma}$ and the symmetric model of Example 1, the approximation

$$F_{ST}^{\text{eq}} \approx \frac{s-1}{2s}\left(\frac{1}{N_c} + \frac{1}{N_e}\cdot\frac{1}{s-1}\sum_{i=2}^{s}\frac{\eta_i^2}{1-\eta_i^2}\right) \tag{43}$$

is accurate for large local population sizes when subpopulations are connected by strong migration. For the island model (43) we insert (39) into (43) and obtain

$$F_{ST}^{\text{eq}} \approx \frac{s-1}{2s\tilde{N}[1-(1-m)^2]}, \tag{44}$$

where

$$\frac{1}{\tilde{N}} = \frac{1-(1-m)^2}{N_c} + \frac{(1-m)^2}{N_e} \tag{45}$$

is a harmonic average of the local census and effective sizes. Formula (44) is accurate when m is not too small. For improved island model approximations of F_{ST}^{eq}, see Hössjer et al. (2013).

6.2 Genetic Drift and Migration

Next we will analyze how the genetic drift term $I = I_{T+t}(\tau)$ and the gene flow term $II = II_{T+t}(\tau)$ behave as $T \to \infty$. From (3), (22), and (37) we deduce that

$$I \xrightarrow{T\to\infty} I_\infty(\tau) = 1 - \left(1 - \frac{1}{2N_{eE}}\right)^\tau \tag{46}$$

and

$$II \xrightarrow{T\to\infty} II_\infty(\tau) = \frac{2\sum_{x,y}((\boldsymbol{v}\boldsymbol{B}^\tau)_x - w_x)w_y r_{xy}}{\sum_{x,y} w_x w_y r_{xy}} \tag{47}$$

when t and $t+\tau$ are kept fixed while $T \to \infty$.

It is shown in Appendix B.3 that the equilibrium gene flow term (47) simplifies to

$$II_\infty(\tau) \approx \sum_{i=2}^{s} \frac{\kappa_i(\kappa_i - \eta_i^\tau \rho_i)}{1-\eta_i^2}\left(\frac{1-\eta_i^2}{N_c} + \frac{\eta_i^2}{N_e}\right) \tag{48}$$

for symmetric migration (cf. Example 1), with $\kappa_i = \boldsymbol{w}\boldsymbol{l}_i^T$ and $\rho_i = \boldsymbol{v}\boldsymbol{l}_i^T$ the coefficients of $\boldsymbol{l}_i$ for $\boldsymbol{w}$ and $\boldsymbol{v}$, when these two weight vectors are expanded as a linear combination of the left eigenvectors $\boldsymbol{l}_i$ of $\boldsymbol{B}$. Formula (48) is accurate when the subpopulations are connected by strong migration. For the island model (38) and (39) we have that $\sum_{i=2}^s \kappa_i^2 = \sum_{x=1}^s w_x^2 - \kappa_1^2 = |\boldsymbol{w}|^2 - 1/s$ and $\sum_{i=2}^s \kappa_i\rho_i = \sum_x w_x v_x - \kappa_1\rho_1 = \boldsymbol{w}\boldsymbol{v}^T - 1/s$. Then (48) simplifies to

$$II_\infty(\tau) \approx \frac{|\boldsymbol{w}|^2 - 1/s - (1-m)^\tau(\boldsymbol{w}\boldsymbol{v}^T - 1/s)}{\tilde{N}[1-(1-m)^2]}, \tag{49}$$

with $\tilde{N}$ as in (45). This formula is accurate as long as m is not too small. In particular, if $1 \le k \le s$ subpopulations receive equal weight $1/k$ at time points t and $t+\tau$, and $\max(2k-s, 0) \le l \le k$ of these overlap, it follows that $|\boldsymbol{w}|^2 = 1/k$ and $\boldsymbol{w}\boldsymbol{v}^T = l/k^2$. Insertion into (49) gives

$$II_{\infty}(\tau) \approx \frac{1/k - 1/s - (1-m)^{\tau}(l/k^2 - 1/s)}{\tilde{N}[1-(1-m)^2]}. \tag{50}$$

Notice in particular that the right hand side of (50) vanishes when $k = l = s$. This corresponds to using equal weights $w_x = v_x = 1/s$ of all subpopulations at both time points t and $t + \tau$, which are the reproductive weights for the island model.

In Sects. 6.3 and 6.4 we will use (46)–(50) in order to derive explicit expressions for the gene diversity and variance effective sizes under migration–drift equilibrium.

6.3 Gene Diversity Effective Size

It follows from (18) and (46) that the gene diversity effective size equals the eigenvalue effective size under migration–drift equilibrium, since

$$N_{eGD} \xrightarrow{T\to\infty} N_{eGD}^{\mathrm{eq}} = N_{eE}. \tag{51}$$

Notice in particular that since the equilibrium limit $I_{\infty}(\tau)$ of the drift term in (46) does not involve the subpopulation weighting scheme $\boldsymbol{w}$, (51) holds regardless which $\boldsymbol{w}$ we use to define N_{eGD}.

6.4 Variance Effective Size

6.4.1 Forward Approach

The two equations (46) and (47) have interesting implications for the asymptotic limit of the forward version of the variance effective size N_{eV} at migration–drift equilibrium. It follows from (20), (21), (46), and (47) that

$$N_{eV} \xrightarrow{T\to\infty} N_{eV}^{\mathrm{eq}} = \frac{1}{2\{1-[(1-1/(2N_{eE}))^{\tau} - II_{\infty}(\tau)]^{1/\tau}\}} \tag{52}$$

for all τ such that $0 < I_{\infty}(\tau) + II_{\infty}(\tau) < 1$, or equivalently that

$$\left(1 - \frac{1}{2N_{eE}}\right)^{\tau} > II_{\infty}(\tau) \tag{53}$$

holds. We may apply (52) to any kind of weighting scheme. Since N_{eVMeta} is based on reproductive weights $\boldsymbol{w} = \boldsymbol{v} = \boldsymbol{\gamma}$, and $\boldsymbol{\gamma} = \boldsymbol{\gamma B}$, it follows from (23) that $II_{T+t}(\tau) = 0$ for any $T \geq 0$, and hence $II_{\infty}(\tau) = 0$. Insertion into (52) gives

$$N_{eVMeta} \xrightarrow{T\to\infty} N_{eVMeta}^{\mathrm{eq}} = N_{eE}. \tag{54}$$

For local subpopulation weights we insert $\boldsymbol{v} = \boldsymbol{w} = \boldsymbol{e}_x$ into the definition of $II_{\infty}(\tau)$ in (47). In conjunction with (52) this gives the equilibrium value N_{eVRx}^{eq} of the realized variance effective size of subpopulation x, for all τ such that (53) holds.

It is proved in Appendix B.4 that the variance effective size at migration–drift equilibrium satisfies

$$N_{eV\boldsymbol{w}\boldsymbol{v}}^{\mathrm{eq}} \leq N_{eV\boldsymbol{w}}^{\mathrm{eq}} \tag{55}$$

for the island model, and subpopulations weights $\boldsymbol{w}$ and $\boldsymbol{v}$ at time points t and $t+\tau$ such that $\boldsymbol{w}\boldsymbol{v}^T \leq |\boldsymbol{w}|^2$, with equality in (55) if and only if $\boldsymbol{w}\boldsymbol{v}^T = |\boldsymbol{w}|^2$. The intuition behind (55) is that $II_\infty(\tau)$ is elevated when different subpopulation weights are used in generations t and $t+\tau$, since the negative correlation II between allele frequency change of the past and present then increases, so that the variance effective size gets smaller. We also verify in Appendix B.4 that

$$N_{eV\boldsymbol{w}}^{\mathrm{eq}} \leq N_{eV\boldsymbol{\gamma}}^{\mathrm{eq}} = N_{eVMeta}^{\mathrm{eq}} = N_{eE} \tag{56}$$

for the symmetric migration models of Example 1, with equality if and only if reproductive weights ($\boldsymbol{w} = \boldsymbol{v} = \boldsymbol{\gamma}$) are used at time points t and $t+\tau$. The intuition behind (56) is that the gene flow term $II_\infty(\tau)$ is positive as soon as non-reproductive weights $\boldsymbol{w} = \boldsymbol{v} \neq \boldsymbol{\gamma}$ are used, so that $N_{eV\boldsymbol{w}}$ gets smaller. We also conjecture that results similar to (55) and (56) hold more generally than for island and symmetric migration models respectively.

It is instructive to illustrate (55) and (56) for an island model where $1 \leq k \leq s$ subpopulations are assigned equal weight $1/k$ at both time points t and $t+\tau$, and that l of these subpopulations overlap. Insertion of the equilibrium migration term $II_\infty(\tau)$ in (50) into (52) yields

$$N_{eV}^{\mathrm{eq}} \approx \frac{1}{2\left\{1 - \left[(1-1/(2N_{eE}))^\tau - \frac{1/k-1/s-(1-m)^\tau(l/k^2-1/s)}{\tilde{N}[1-(1-m)^2]}\right]^{1/\tau}\right\}}. \tag{57}$$

This formula shows very explicitly how much N_{eV}^{eq} differs from N_{eE}, as a function of k and l. For fixed k, N_{eV}^{eq} is maximized in (57) when the same subpopulation weights are used at both time points ($l = k$), in agreement with (55). When $k = l$, we notice that N_{eV}^{eq} attains its maximum N_{eE} when reproductive weights are used at both time points, which corresponds to $k = s$ and $\boldsymbol{w} = \boldsymbol{\gamma} = \mathbf{1}_s^T/s$, in agreement with (56).

6.4.2 Intermediate Approach

For the intermediate approach, we have, analogously to (52), that the variance effective size at equilibrium is

$$N_{eV}^{\mathrm{int}} \xrightarrow{T\to\infty} N_{eV}^{\mathrm{int,eq}} = \frac{1}{2\left\{1 - \left[\frac{(1-1/(2N_{eE}))^\tau - \frac{1}{2}II_\infty(\tau)}{1+\frac{1}{2}II_\infty(\tau)}\right]^{1/\tau}\right\}}, \tag{58}$$

for all τ such that

$$\left(1-\frac{1}{2N_{eE}}\right)^{\tau} > \frac{1}{2}II_{\infty}(\tau), \tag{59}$$

which is a less stringent condition than (53) for the variance effective size to exist. Since $II_{\infty}(\tau)=0$ for reproductive weights, it follows that $N_{eVMeta}^{\text{int,eq}}$ converges to N_{eE} as migration–drift equilibrium is approached, as in (54). The local realized variance effective size $N_{eVRx}^{\text{int,eq}}$ at equilibrium is obtained by inserting $\boldsymbol{w}=\boldsymbol{v}=\boldsymbol{e}_x$ into the definition of $II_{\infty}(\tau)$ in (58). Formulas (55) and (56) hold for the intermediate version of the variance effective size as well, and explicit expressions of $N_{eV}^{\text{int,eq}}$ for the island model are obtained by inserting (50) into (58).

6.4.3 Backward Approach

For the backward approach, we find that the variance effective size at equilibrium exists for time intervals of any length τ. This equilibrium value

$$N_{eV}^{\text{back}} \xrightarrow{T\to\infty} N_{eV}^{\text{back,eq}} = \frac{1}{2\left\{1-\frac{1-1/(2N_{eE})}{[1+II_{\infty}(\tau)]^{1/\tau}}\right\}} \tag{60}$$

is derived in the same way as (52) and (58). For local subpopulation weights we insert $\boldsymbol{w}=\boldsymbol{v}=\boldsymbol{e}_x$ into the definition of $II_{\infty}(\tau)$ in Eq. (60) in order to obtain $N_{eV,Rx}^{\text{back,eq}}$. Formulas (55) and (56) hold for the backward version of the variance effective size as well, and explicit expressions of $N_{eV}^{\text{back,eq}}$ for the island model are obtained by inserting (50) into (60).

7 The Length of the Time Interval

In this section we analyze how the length τ of the time interval impacts the gene diversity and variance effective sizes. We will focus on the two extreme scenarios of consecutive generations ($\tau=1$) and long time intervals ($\tau\to\infty$).

7.1 Consecutive Generations

For ease of notation, we will sometimes write $I_{T+t}(\tau)=I(\tau)$ and $II_{T+t}(\tau)=II(\tau)$ for the genetic drift and gene flow terms that appear in the definitions of the gene diversity and variance effective sizes. When these effective sizes reflect changes between two consecutive generations ($\tau=1$), formulas (18), (21), (28), and (33) simplify to

$$N_{eGD} = \frac{1}{2I(1)} \overset{\text{eq}}{=} N_{eE}, \tag{61}$$

$$N_{eV} = \frac{1}{2[I(1) + II(1)]} \stackrel{\text{eq}}{=} \frac{1}{\frac{1}{N_{eE}} + 2II_{\infty}(1)}, \tag{62}$$

$$N_{eV}^{\text{int}} = \frac{1 + \frac{1}{2}II(1)}{2[I(1) + II(1)]} \stackrel{\text{eq}}{=} \frac{1 + \frac{1}{2}II_{\infty}(1)}{\frac{1}{N_{eE}} + 2II_{\infty}(1)}, \tag{63}$$

and

$$N_{eV}^{\text{back}} = \frac{1 + II(1)}{2[I(1) + II(1)]} \stackrel{\text{eq}}{=} \frac{1 + II_{\infty}(1)}{\frac{1}{N_{eE}} + 2II_{\infty}(1)} \tag{64}$$

respectively, where the right hand sides of (61)–(64) refer to migration–drift equilibrium, with $I_{\infty}(1)$ and $II_{\infty}(1)$ the drift and gene flow terms in (46) and (47) at equilibrium, for two consecutive generations. Typically the gene flow term is small ($II(1) \ll 1$) unless there is much migration between the subpopulations and a large amount of subpopulation differentiation at time t. Consequently, for most scenarios of practical interest the three versions of variance effective size are practically the same,

$$\frac{1}{2[I(1) + II(1)]} = N_{eV} \approx N_{eV}^{\text{int}} \approx N_{eV}^{\text{back}}, \tag{65}$$

Table 2 Values of the realized local variance effective size N_{eVRx} at migration–drift equilibrium for a time interval of length $\tau = 1$, so that the same subpopulation x receives full weight at the two end points of the interval

	$N_{cx} = 50$			$N_{cx} = 500$		
	For	Int	Back	For	Int	Back
0.1	47.2960	47.5232	47.7504	56.4109	56.6337	56.8566
0.2	45.0331	45.2609	45.4888	64.3622	64.5805	64.7988
0.3	42.7467	42.9755	43.2043	74.2336	74.4468	74.6600
0.4	40.4368	40.6667	40.8966	86.5645	86.7714	86.9783
0.5	38.1032	38.3342	38.5652	101.9387	102.1379	102.3371
0.6	35.7455	35.9777	36.2098	120.7432	120.9329	121.1227
0.7	33.3633	33.5967	33.8300	142.4849	142.6637	142.8426
0.8	30.9564	31.1909	31.4254	164.3497	164.5176	164.6854
0.9	28.5242	28.7599	28.9956	179.5012	179.6615	179.8217
1.0	26.0664	26.3033	26.5403	178.4566	178.6174	178.7781

An island model with $s = 10$ subpopulations is used, with local effective size $N_{ex} = 50$ under isolation, local census size N_{cx} and migration parameter m (where $B_{xy} = m/s$ when $x \neq y$ and $B_{xx} = 1 - (s-1)m/s$). The three methods of computing N_{eVRx} refer to the forward approach (= For, the right hand side of (62)), the intermediate approach (= Int, the right hand side of (63)), and the backward approach (= Back, the right hand side of (64)). A more explicit approximation of N_{eVRx}, for the forward approach, appears in (66)

Table 3 Values of the realized local variance effective size N_{eVRxy} at migration–drift equilibrium, for a time interval of length $\tau = 1$, so that different subpopulations x and y receive full weight at the two end points of the interval

m	$N_{cx} = 50$			$N_{cx} = 500$		
	For	Int	Back	For	Int	Back
0.1	4.6878	4.9355	5.1833	5.6902	5.9375	6.1847
0.2	8.9166	9.1622	9.4078	13.1853	13.4288	13.6723
0.3	12.6738	12.9175	13.1612	23.1186	23.3572	23.5957
0.4	15.9668	16.2089	16.4509	36.3781	36.6100	36.8419
0.5	18.8007	19.0413	19.2820	54.0715	54.2945	54.5176
0.6	21.1778	21.4172	21.6567	77.2921	77.5035	77.7149
0.7	23.0977	23.3362	23.5746	106.2835	106.4804	106.6774
0.8	24.5571	24.7948	25.0326	138.5156	138.6964	138.8772
0.9	25.5498	25.7870	26.0242	166.3374	166.5042	166.6710
1.0	26.0664	26.3033	26.5403	178.4566	178.6174	178.7781

An island model with $s = 10$ subpopulations is used, with local effective size $N_{ex} = 50$ under isolation, local census size N_{cx} and migration parameter m (where $B_{xy} = m/s$ when $x \neq y$ and $B_{xx} = 1 - (s-1)m/s$). The three methods of computing N_{eVRxy} refer to the forward approach (=For, the right hand side of (62)), the intermediate approach (=Int, the right hand side of (63)), and the backward approach (=Back, the right hand side of (64)). A more explicit approximation of N_{eVRxy}, for the forward approach, appears in (67)

when the expected squared allele frequency change between two consecutive generations is analyzed. This is illustrated in Tables 2 and 3 for the realized local variance effective size of an island model with $s = 10$ subpopulations at migration–drift equilibrium, corresponding to the right hand side of (62)–(64). Whereas the same subpopulation weights are used at both time points in Table 2 ($\boldsymbol{w} = \boldsymbol{v} = \boldsymbol{e}_x$ or $k = l = 1$), this is not the case in Table 3 ($\boldsymbol{w} = \boldsymbol{e}_x$, $\boldsymbol{v} = \boldsymbol{e}_y$, $x \neq y$ or $k = 1, l = 0$). Note in particular that all three versions of the realized local variance effective size depend strongly on the local census size. This phenomenon is discussed in Ryman et al. (2023), and in the present framework in can be explained as follows: The term $II_\infty(1)$ is approximated by (49) and (50) for the island model and it depends on the amount of migration into x or y from the other subpopulations as well as the amount of subpopulation differentiation F_{ST}^{eq} in (44). The larger the migration rate and the local census size are, the smaller is the amount of subpopulation differentiation, and the smaller is the gene flow term $II_\infty(1)$ at equilibrium, so that the variance effective size approaches the eigenvalue effective size.

A more analytical interpretation of the results of Table 2 is obtained by inserting $\tau = 1$ and $\boldsymbol{w} = \boldsymbol{v} = \boldsymbol{e}_x$ into (49) and the right hand side of (62). This yields

$$N_{eVRx}^{\text{eq}} \approx \frac{1}{\frac{1}{N_{eE}} + \frac{2(1-1/s)}{(2-m)\tilde{N}}} \overset{(44)}{\approx} \frac{1}{\frac{1}{N_{eE}} + 4mF_{ST}^{\text{eq}}}. \tag{66}$$

On the other hand, in order to approximate the results of Table 3, we insert $\tau = 1$, $\boldsymbol{w} = \boldsymbol{e}_x$, and $\boldsymbol{v} = \boldsymbol{e}_y$ into the right hand side of (62). This yields

$$N_{eVRxy}^{\mathrm{eq}} \approx \frac{1}{\frac{1}{N_{eE}} + \frac{2(1-m/s)}{(2-m)m\tilde{N}}} \overset{(44)}{\approx} \frac{1}{\frac{1}{N_{eE}} + 4F_{ST}^{\mathrm{eq}} \frac{s-m}{s-1}}. \tag{67}$$

Formulas (66) and (67) are also obtained from (57), with $\tau = 1$, $k = 1$, and $l = 1$ or $l = 0$ respectively. They are accurate when the migration rate m is not too small. In particular, under panmixia it follows from (57) that

$$N_{eV}^{\mathrm{eq}} \overset{m=1}{=} \frac{1}{\frac{1}{N_{eE}} + \frac{2(1-1/s)}{N_c}}, \tag{68}$$

regardless of the loal weight vectors $\boldsymbol{w} = \boldsymbol{e}_x$ and $\boldsymbol{v} = \boldsymbol{e}_y$ of the subpopulations at time points t and $t+1$. Note that (68) is the limit of (66) and (67) when $m \to 1$, and that (68) approaches N_{eE} when $N_c \to \infty$.

7.2 Long Time Intervals

When the length τ of the time interval gets large, it may happen that the standardized allele frequency change of the forward and intermediate versions of the variance effective size satisfy $Q(\tau) \geq 1$, so that the corresponding effective size equals 0 or $-\infty$. In this subsection we will provide formulas for the maximal length $\tau_{\max,Q}$ of the time interval for which each type Q of effective size exists under migration–drift equilibrium. Since the gene diversity effective size equals the eigenvalue effective size at equilibrium, for time intervals of any length (cf. (51)), it follows that

$$\tau_{\max,GD} = \infty.$$

For the forward version of the variance effective size, it follows from (53) that

$$\tau_{\max,V} \approx \log[II_\infty^{-1}] \cdot 2N_{eE}, \tag{69}$$

where the right hand side is interpreted as plus infinity whenever

$$II_\infty = \lim_{\tau\to\infty} II_\infty(\tau) = \frac{2\sum_{x,y}(\gamma_x - w_x)w_y r_{xy}}{\sum_{x,y} w_x w_y r_{xy}} \tag{70}$$

is zero or negative. The approximation in (69) is accurate for large N_{eE}. It implies that N_{eV}^{eq} exists for time intervals up to a maximal length that is proportional to N_{eE}. For the intermediate version of the variance effective size, we similarly deduce

$$\tau_{\max,V}^{\mathrm{int}} \approx \log\left[2II_\infty^{-1}\right] \cdot 2N_{eE} \tag{71}$$

from formula (59). We recall from (60) that the backward version of the variance effective size exists at equilibrium for time intervals of any length, so that

$$\tau_{\max,V}^{\mathrm{back}} = \infty.$$

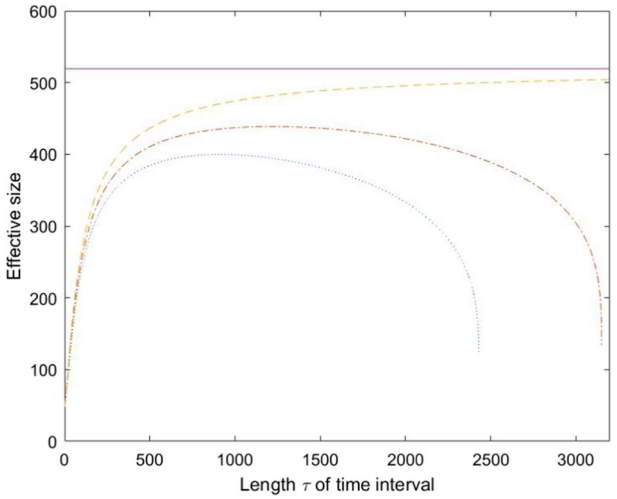

Fig. 1 The figure plots effective sizes for an island model with $s = 10$, $N_{ex} = N_{cx} = 50$ and $m = 0.1$, when $t = 0$ corresponds to migration–drift equilibrium ($T \to \infty$). The horizontal solid line corresponds to $N_{eE} = 519.28$. The three curves correspond to N_{eVRx} (dotted), N^{int}_{eVRx} (dash-dotted) and N^{back}_{eVRx} (dashed) for intervals $[0, \tau]$ of increasing length. N_{eVRx} increases with τ at first, then it starts to drop until $\tau = \tau_{\max} = 2431$, and for longer intervals N_{eVRx} does not exist. In comparison, formula (69) predicts $\tau_{\max,\text{V}} = \log(II_{\infty}^{-1}) \cdot 2N_{eE} = 2432.8$. In a similar fashion N^{int}_{eVRx} increases with τ at first, then it starts to drop until $\tau = \tau_{\max} = 3151$, and after this generation N^{int}_{eVRx} does not exist. In comparison, formula (71) predicts $\tau^{\text{int}}_{\max,V} = \log(2II_{\infty}^{-1}) \cdot 2N_{eE} = 3152.7$. On the other hand, N^{back}_{eVRx} increases monotonically to N_{eE} as $\tau \to \infty$

In particular, by increasing the length of the time interval in (60) we find that

$$N^{\text{back,eq}}_{eV} \xrightarrow{\tau \to \infty} N_{eE}, \tag{72}$$

for all types of subpopulation weights $\boldsymbol{w}$.

Figure 1 illustrates the eigenvalue effective size N_{eE}, and the forward, intermediate, and backward versions of the realized local variance effective size over time intervals $[0, \tau]$ of increasing length when the population is at migration–drift equilibrium. The model is an island model with $s = 10$ subpopulations and the migration rate equals $m = 0.1$. It can be seen that N_{eVRx} and N^{int}_{eVRx} initially increase as τ grows, until they reach a maximum, start to decline and eventually do not exist. In contrast, N^{back}_{eVRx} always exists and increases monotonically to N_{eE} as the length τ of the time interval grows, in agreement with (72). The corresponding variance effective sizes N_{eVMeta}, N^{int}_{eVMeta} and N^{back}_{eVMeta} of the metapopulation, based on equal subpopulation weights $w_x = 1/s$, equal N_{eE} for all values of τ.

The three realized local variance effective sizes of Fig. 1 are almost the same for time intervals of length up to 200–300 generations, which is at least tenfold the time span typically employed in the context of genetic conservation. However, it is shown in Appendix A that for a small and subdivided population, the three effective sizes may differ substantially for time intervals of length 5–10 generations. More

generally, the value of τ for which the three effective sizes significantly start to differ is proportional to N_{eE}. For populations that are either very small locally or experience a severe bottleneck, it may therefore be of interest to use the most stable version N_{eVRx}^{back} of the realized local variance effective size.

8 Estimation of Effective Sizes

In this section we will investigate how the length τ of the time interval impacts the accuracy of an estimator of the gene diversity and variance effective sizes at equilibrium (N_{eQ}^{eq}, $Q \in \{GD, V\}$). Our theoretical analysis is complementary to the simulation results of Luikart et al. (1999), where interval lengths with maximal accuracy, for a variance effective size estimator, were derived for a population going through a bottleneck. Here we stick to the model introduced in Sect. 2, with time-invariant population sizes of all subpopulations. We start by introducing

$$Q(\tau) = Q^{\text{eq}}(\tau) = g\left(\frac{1}{2N_{eQ}^{\text{eq}}}\right) = 1 - \left(1 - \frac{1}{2N_{eQ}^{\text{eq}}}\right)^{\tau},$$

the value, at migration–drift equilibrium, of the quantity Q used to define each effective size. More specifically, in this section $Q(\tau)$ corresponds to the limit, when $T \to \infty$, of the quantities that appear in (18), (20), (25), and (30) respectively. A necessary requirement for N_{eQ}^{eq} to exist is that $0 < Q(\tau) < 1$. Recall from Sect. 7.2 that this is not always the case for the forward and intermediate versions of the variance effective size.

In order to estimate N_{eQ}^{eq} from data, let $\hat{Q}(\tau) = Q(\tau) + \varepsilon$ be an estimate of $Q(\tau)$, based on samples of sizes n_t and $n_{t+\tau}$ at time points t and $t + \tau$. We will assume that the estimation error ε of $\hat{Q}(\tau)$ is a random variable with $E(\varepsilon) = 0$ and $\text{Var}\,(\varepsilon) = \sigma^2$. Typically σ^2 is inversely proportional to the number of biallelic markers used to estimate $Q(\tau)$, with a proportionality constant that is a monotone increasing function of $1/(2n_t)$ and $1/(2n_{t+\tau})$ (Waples 1989). Our objective is to estimate the asymptotic amount of genetic drift

$$Q = \frac{1}{2N_{eQ}^{\text{eq}}} = h(Q(\tau)) \tag{73}$$

per generation at equilibrium, where

$$h(Q(\tau)) = g^{-1}(Q(\tau)) = 1 - (1 - Q(\tau))^{1/\tau}$$

is the inverse of g. By a first order Taylor expansion of h, it can be seen that the error of the estimate $\hat{Q} = h(\hat{Q}(\tau))$ has an approximate variance

$$\text{Var}\,(\hat{Q}) \approx \sigma^2 \left(\frac{dh(Q(\tau))}{dQ(\tau)}\right)^2 = \sigma^2 \left\{\frac{1}{\tau}[1 - Q(\tau)]^{\frac{1}{\tau}-1}\right\}^2. \tag{74}$$

Our objective is to express Var $(\hat{Q})$ as a function of τ for each quantity Q and weighting scheme $\boldsymbol{w}$. The variance in (74) will initially decrease with τ, since for short time intervals $Q(\tau) \ll 1$ and consequently

$$\text{Var}\,(\hat{Q}) \approx \frac{\sigma^2}{\tau^2}. \tag{75}$$

When τ gets larger and $Q(\tau)$ approaches 1, the variance in (74) will reach a minimum and then start to increase. For this reason it is of interest to find approximate expressions for the interval length

$$\begin{aligned} \tau_{\text{opt},Q} &= \arg\ \min_\tau\ \text{Var}\,(\hat{Q}) \\ &= \arg\ \min_\tau\, dh(Q(\tau))/dQ(\tau) \\ &= \arg\ \min_\tau\, \tfrac{1}{\tau}[1-Q(\tau)]^{\frac{1}{\tau}-1} \end{aligned} \tag{76}$$

that minimizes the estimation variance in (74). As we will find below, Var $(\hat{Q})$ is a function of N_{eE} and the equilibrium gene flow term $II_\infty(\tau)$, defined in (47). It turns out that the optimal time interval will have a length $\tau_{\text{opt},Q}$ that is proportional to N_{eE}. For a system with strong migration between its subpopulations (Nagylaki 1980) $II_\infty(\tau)$ approaches the asymptotic limit (70) so quickly that the length of the transient period is small in comparison to N_{eE}. For a population with strong migration we will therefore approximate $\tau_{\text{opt},Q}$ by minimizing a simplified version of $dh(Q(\tau))/dQ(\tau)$ with respect to τ, where $II_\infty(\tau)$ is replaced by the constant II_∞ in (70).

As a complement to (76) we also define

$$\tau_{C,Q} = \min\{\tau; \sqrt{\frac{\text{Var}\,(\hat{Q})}{\sigma^2}} \geq C\} - 1 \tag{77}$$

as the largest value of τ for which the standard deviation of the estimate of Q has not exceeded σ by a factor of at least $C > 1$. In particular, $\tau_{\infty,Q}$ is closely related to $\tau_{\max,Q}$.

8.1 Gene Diversity Effective Size

For the gene diversity effective size we recall from (18) and (46) that

$$Q(\tau) = I_\infty(\tau) = 1 - \left(1 - \frac{1}{2N_{eE}}\right)^\tau.$$

Insertion of this equation into (74) yields

$$\frac{dh(Q(\tau))}{dQ(\tau)} = \frac{1}{\tau}\left[1 - I_\infty(\tau)\right]^{\frac{1}{\tau}-1} = \frac{1}{\tau}\left(1 - \frac{1}{2N_{eE}}\right)^{1-\tau}. \tag{78}$$

Minimizing (78) with respect to τ, we find that the optimal length of the time interval, when estimating the gene diversity effective size, is

$$\tau_{\text{opt},GD} = 2N_{eE}. \tag{79}$$

8.2 Variance Effective Size

8.2.1 Forward Approach

The quantity $Q(\tau)$ of the forward version of the variance effective size is obtained from (20) and (46) and (47). The resulting formula

$$Q(\tau) = 1 - \left(1 - \frac{1}{2N_{eE}}\right)^{\tau} + II_{\infty}(\tau) \tag{80}$$

leads to

$$\frac{dh(Q(\tau))}{dQ(\tau)} = \frac{1}{\tau}[1 - Q(\tau)]^{\frac{1}{\tau}-1} = \frac{1}{\tau}\left[\left(1 - \frac{1}{2N_{eE}}\right)^{\tau} - II_{\infty}(\tau)\right]^{\frac{1}{\tau}-1}. \tag{81}$$

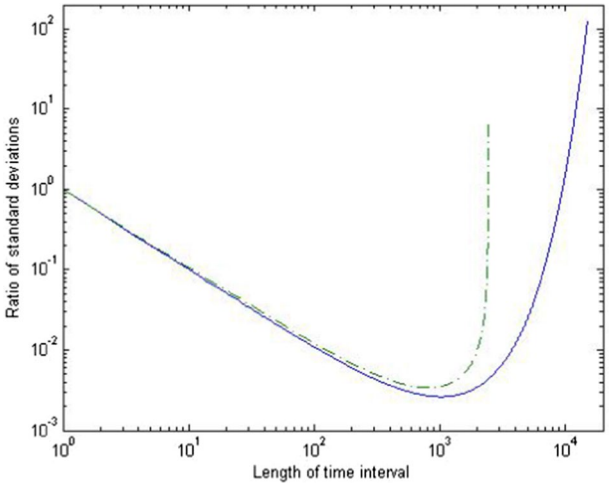

Fig. 2 Using the forward definition of variance effective size, the figure shows a log–log plot of the normalized standard deviation $\text{Var}(\hat{Q})^{1/2}/\sigma$ for estimating $Q = 1/(2N_{eV}^{\text{eq}})$, the average amount of genetic drift per generation at equilibrium, for time intervals $[0, \tau]$. The population model is the same as in Fig. 1, and the solid and dash-dotted curves correspond to $N_{eVRMeta}^{\text{eq}}$ and N_{eVRx}^{eq} respectively. The solid curve has $\tau_{1.5} = 9980$, $\tau_2 = 10313$, $\tau_3 = 10780$, $\tau_4 = 11110$, and $\tau_5 = 11365$ (cf. (77)), whereas the optimal interval has length $\tau_{\text{opt}} = 1038$ (cf. (76)). For comparison, formula (83) gives $d_{\text{opt}} = 1.000$ and $d_{\text{opt}} 2N_{eE} = 1038.6$. The corresponding values of the dash-dotted curve are $\tau_{1.5} = 2428$, $\tau_2 = 2429$, $\tau_3 = \tau_4 = 2430$, $\tau_5 = 2431$, and $\tau_{\text{opt}} = 819$, $d_{\text{opt}} = 0.7886$, and $d_{\text{opt}} 2N_{eE} = 819.0$

Equating the derivative with respect to τ to 0, of a simplified version of (81) (where $II_\infty(\tau)$ is replaced by II_∞), and assuming N_{eV} is large, it can be shown that

$$\tau_{\text{opt},V} \approx d_{\text{opt},V} \cdot 2N_{eE} \tag{82}$$

whenever $II_\infty \geq 0$, where $d_{\text{opt},V} = d_{\text{opt},V}(II_\infty)$ solves the equation

$$d_{\text{opt},V} + II_\infty e^{d_{\text{opt},V}} = 1. \tag{83}$$

We interpret II_∞ as a number that quantifies how much migration between subpopulations impacts the variance of allele frequency change. It can be seen from (83) that $d_{\text{opt},V}$ is a decreasing function of II_∞, with $d_{\text{opt},V} = 1$ for N^{eq}_{eVMeta} and $II_\infty = 0$, whereas $d_{\text{opt},V} \to 0$ as $II_\infty \to 1$. It follows from (83) that $d_{\text{opt},V} < \log(II_\infty^{-1})$, and consequently, the optimal interval (76) is shorter than the length $\tau_{\max,V}$ of the maximal interval in (69) for which N^{eq}_{eV} exists.

Figure 2 is a log–log plot of the normalized standard deviation $\text{Var}\,(\hat{Q})^{1/2}/\sigma$ of $\hat{Q}$ as a function of τ for an island model with $s = 10$ subpopulations, when estimating the variance effective size of the metapopulation and a local population respectively. The linear decay to the left of the figure, for smaller τ, corresponds to $\text{Var}\,(\hat{Q})^{1/2}$ being inversely proportional to τ for intervals of short length, in agreement with (75). Note in particular the vertical asymptote of the dash-dotted curve. This corresponds to the fact that $\text{Var}\,(\hat{Q})$ diverges when τ approaches the length of intervals for which N^{eq}_{eVRx} is no longer defined (cf. Fig. 1).

8.2.2 Intermediate Approach

For the intermediate definition of the variance effective size we proceed similarly as in Sect. 8.2.1. It follows from (25), (28), and (46) and (47) that

$$Q(\tau) = \frac{1 - \left(1 - \frac{1}{2N_{eE}}\right)^{\tau} + II_\infty(\tau)}{1 + \frac{1}{2}II_\infty(\tau)}, \tag{84}$$

which leads to

$$\frac{dh(Q(\tau))}{dQ(\tau)} = \frac{1}{\tau}[1 - Q(\tau)]^{\frac{1}{\tau}-1} = \frac{1}{\tau}\left[\frac{\left(1 - \frac{1}{2N_{eE}}\right)^{\tau} - \frac{1}{2}II_\infty(\tau)}{1 + \frac{1}{2}II_\infty(\tau)}\right]^{\frac{1}{\tau}-1}. \tag{85}$$

Replacing $II_\infty(\tau)$ in (85) by II_∞ and minimizing with respect to τ, it follows that

$$\tau^{\text{int}}_{\text{opt},V} \approx d^{\text{int}}_{\text{opt},V} \cdot 2N_{eE}, \tag{86}$$

with

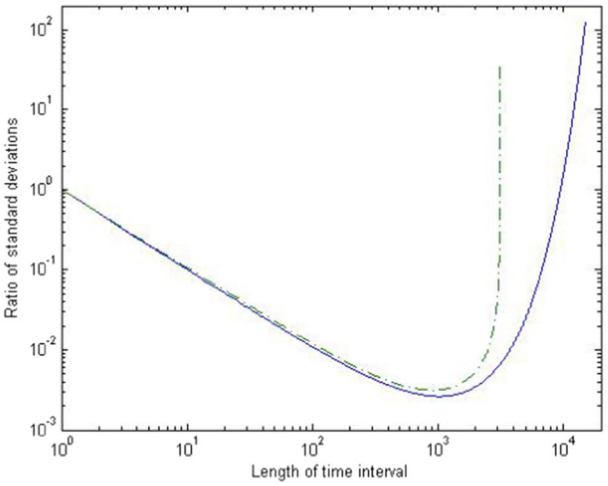

Fig. 3 Using the intermediate definition of variance effective size, the figure shows a log–log plot of the normalized standard deviation $\mathrm{Var}\,(\hat{Q})^{1/2}/\sigma$ for estimating $Q = 1/(2N_{eV}^{\mathrm{int,eq}})$, the average amount of genetic drift per generation at equilibrium, for time intervals $[0, \tau]$. The population model is the same as in Fig. 1, and the solid and dash-dotted curves correspond to $N_{eVRMeta}^{\mathrm{int,eq}}$ and $N_{eVRx}^{\mathrm{int,eq}}$ respectively. The solid curve has $\tau_{1.5} = 9980$, $\tau_2 = 10313$, $\tau_3 = 10780$, $\tau_4 = 11110$, and $\tau_5 = 11365$ (cf. (77)), whereas the optimal interval has length $\tau_{\mathrm{opt}} = 1038$ (cf. (76)). For comparison, formula (83) gives $d_{\mathrm{opt}} = 1.000$ and $d_{\mathrm{opt}} 2N_{eE} = 1038.6$. The corresponding values of the dash-dotted curve are $\tau_{1.5} = 3146$, $\tau_2 = 3147$, $\tau_3 = 3148$, $\tau_4 = \tau_5 = 3149$, and $\tau_{\mathrm{opt}} = 917$, $d_{\mathrm{opt}} = 0.8837$, and $d_{\mathrm{opt}} 2N_{eE} = 917.8$

$$d_{\mathrm{opt},V}^{\mathrm{int}} + \frac{1}{2} II_\infty e^{d_{\mathrm{opt},V}^{\mathrm{int}}} = 1. \tag{87}$$

Notice that $d_{\mathrm{opt}}^{\mathrm{int},V} = 1$ when $II_\infty = 0$, whereas $d_{\mathrm{opt}}^{\mathrm{int},V} < 1$ is larger than (83) whenever $II_\infty > 0$. This verifies that it is possible to estimate the variance effective size with high accuracy over longer time intervals when the intermediate approach is used, compared to using the forward approach.

Figure 3 illustrates $\mathrm{Var}\,(\hat{Q})^{1/2}/\sigma$ for an island model with $s = 10$ subpopulations. The linear decay to the left of the figure, for smaller τ, corresponds to $\mathrm{Var}\,(\hat{Q})^{1/2}$ being inversely proportional to τ for intervals of short length, in agreement with (75). The vertical asymptote of the dash-dotted curve corresponds to the fact that $\mathrm{Var}\,(\hat{Q})$ diverges when τ approaches the length of intervals for which $N_{eVRx}^{\mathrm{int,eq}}$ is no longer defined (cf. Fig. 1).

8.2.3 Backward Approach

In order to find $Q(\tau)$ for the backward definition of the variance effective size we combine (30), (33), and (46) and (47). This leads to

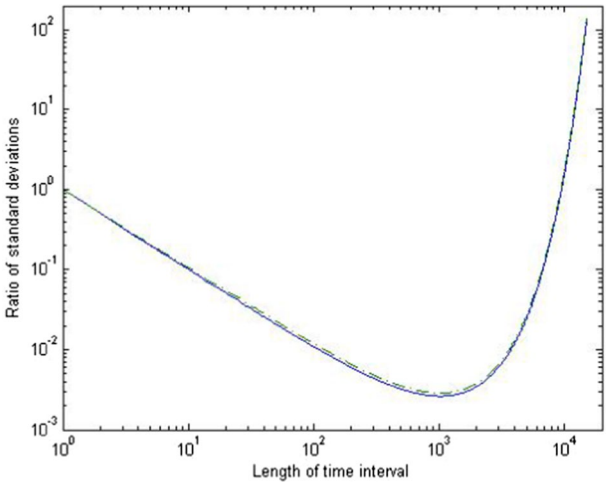

Fig. 4 Using the backward definition of variance effective size, the figure shows a log–log plot of the normalized standard deviation $\mathrm{Var}\,(\hat{Q})^{1/2}/\sigma$ for estimating $Q = 1/(2N_{eV}^{\mathrm{back,eq}})$, the average amount of genetic drift per generation at equilibrium, for time intervals $[0, \tau]$. The population model is the same as in Fig. 1, and the solid and dash-dotted curves correspond to $N_{eVRMeta}^{\mathrm{back,eq}}$ and $N_{eVRx}^{\mathrm{back,eq}}$ respectively. The solid curve has $\tau_{1.5} = 9980$, $\tau_2 = 10313$, $\tau_3 = 10780$, $\tau_4 = 11110$, and $\tau_5 = 11365$ (cf. (77)), whereas the optimal interval has length $\tau_{\mathrm{opt}} = 1038$ (cf. (76)). The corresponding values of the dash-dotted curve are $\tau_{1.5} = 9874$, $\tau_2 = 10207$, $\tau_3 = 10674$, $\tau_4 = 11005$, $\tau_5 = 11260$, and $\tau_{\mathrm{opt}} = 1038$. For comparison, formula (83) gives $d_{\mathrm{opt}} = 1.000$ and $d_{\mathrm{opt}} 2N_{eE} = 1038.6$ for both curves

$$Q(\tau) = \frac{1 - \left(1 - \frac{1}{2N_{eE}}\right)^{\tau} + II_{\infty}(\tau)}{1 + II_{\infty}(\tau)} \tag{88}$$

and

$$\frac{dh(Q(\tau))}{dQ(\tau)} = \frac{1}{\tau}[1 - Q(\tau)]^{\frac{1}{\tau}-1} = \frac{1}{\tau}\frac{\left(1 - \frac{1}{2N_{eE}}\right)^{1-\tau}}{(1 + II_{\infty}(\tau))^{\frac{1}{\tau}-1}}. \tag{89}$$

It can be seen that the length $\tau_{\mathrm{opt},V}^{\mathrm{back}} = d_{\mathrm{opt},V}^{\mathrm{back}} \cdot 2N_{eE}$ that minimizes (89) is proportional to $2N_{eE}$, as in (76). For large N_{eE}, the proportionality constant is $d_{\mathrm{opt},V}^{\mathrm{back}} \approx 1$. Consequently, the length of the optimal interval for the backward version of the variance effective size is

$$\tau_{\mathrm{opt},V}^{\mathrm{back}} \approx 2N_{eE}, \tag{90}$$

similarly as for the gene diversity effective size in (79). Comparing (90) with (83) and (87) we find that the optimal time interval of the backward approach is longer than the corresponding optimal intervals of the forward and intermediate definitions of the variance effective size.

Figure 4 illustrates $\text{Var}\,(\hat{Q})^{1/2}/\sigma$ for an island model with $s = 10$ subpopulations. The linear decay to the left of the figure, for smaller τ, corresponds to $\text{Var}\,(\hat{Q})^{1/2}$ being inversely proportional to τ for intervals of short length, in agreement with (75).

9 Estimation of Variance Effective Size from a Real Data Set

In order to illustrate how the variance effective size depends on the chosen subpopulation weights, in this section we analyze a genetic data set of brown trout (*Salmo trutta*) from the Swedish lake Ånnjön. This data set is part of a large longitudinal study comprising 27 different lakes that are located in protected areas of Jämtland County in the central part of Sweden (cf. Andersson et al. (2022) for more details). Biallelic markers are sampled from 96 distinct loci, scattered along the whole genome (all 40 chromosomes) of brown trout, at two time points, corresponding to data that was collected in 1976 and 2017 respectively. Using estimates of the generation time of brown trout, it is assumed that these two time points are approximately $\tau = 6$ generations apart. The Structure software (v.2.3.4; Pritchard et al. 2000; Falush et al. 2003) was used to identify $s = 3$ cryptic subpopulations within Ånnjön.

The variance effective size is estimated as in Jorde and Ryman (2007). This estimator is defined for a homogeneous population. Its properties for subdivided populations, where the allele frequency at each time point and locus is a weighted average of allele frequencies from all subpopulations, were studied in Ryman et al. (2014, 2023). As mentioned in Sect. 5.3.2, the JR07-estimator targets the intermediate version N_{eV}^{int} of the variance effective size. We will write $\hat{N}_{eV\boldsymbol{wv}}^{\text{int}}$ to denote the version of the JR07-estimator that makes use of subpopulation weights $\boldsymbol{w}$ and $\boldsymbol{v}$ at the two time points at which data was collected. It is based on estimates

$$\begin{aligned} \hat{p}_{tl} &= \textstyle\sum_{x=1}^{3} w_x \hat{p}_{txl}, \\ \hat{p}_{t+\tau,l} &= \textstyle\sum_{x=1}^{3} v_x \hat{p}_{t+\tau,xl}, \end{aligned} \tag{91}$$

of the subpopulation weighted allele frequencies at loci $l = 1, \ldots, L = 96$ and time points t and $t + \tau = t + 6$ respectively. Here $\hat{p}_{txl}$ refers to the estimated allele frequency at locus l in subpopulation x at time t, based on a sample of size n_{tx}. In order to define $\hat{N}_{eV\boldsymbol{wv}}^{\text{int}}$ we also need to introduce sample sizes n_t and $n_{t+\tau}$ at time t and $t + \tau$. To this end, we use subpopulation weighted harmonic averages

$$\begin{aligned} n_t &= 1/\textstyle\sum_{x=1}^{3} (w_x^2/n_{tx}), \\ n_{t+\tau} &= 1/\textstyle\sum_{x=1}^{3} (v_x^2/n_{t+\tau,x}) \end{aligned} \tag{92}$$

of the subpopulation specific sample sizes. The rationale for (92) is that $\text{Var}\,(\hat{p}_{txl}) = p_{txl}(1 - p_{txl})/(2n_{tx})$, and therefore the variances

$$\begin{aligned} \text{Var}\,(\hat{p}_{tl}) &= \textstyle\sum_x w_x^2\, \text{Var}\,(\hat{p}_{txl}) \approx p_{tl}(1 - p_{tl})/(2n_t), \\ \text{Var}\,(\hat{p}_{t+\tau,l}) &= \textstyle\sum_x v_x^2\, \text{Var}\,(\hat{p}_{t+\tau,xl}) \approx p_{t+\tau,l}(1 - p_{t+\tau,l})/(2n_{t+\tau}), \end{aligned}$$

Table 4 Estimated variance effective sizes $\hat{N}^{\text{int}}_{eV\boldsymbol{wv}}$, based on subpopulation weights $\boldsymbol{w}$ and $\boldsymbol{v}$ at time points t and $t+6$, for the brown trout data set of lake Ånnjön, with $s = 3$ cryptic subpopulations

Subpopulation weight scenario			$\hat{N}^{\text{int}}_{eV\boldsymbol{wv}}$
Type	$\boldsymbol{w}$	$\boldsymbol{v}$	
Sample sizes	$(n_{t1}, n_{t2}, n_{t3})/C_1$	$(n_{t+6,1}, n_{t+6,2}, n_{t+6,3})/C_2$	207
Equal	(0.333,0.333,0.333)	$= \boldsymbol{w}$	335
Mostly 1	(1.000,0.000,0.000)	$= \boldsymbol{w}$	155
	(0.833,0.083,0.083)	$= \boldsymbol{w}$	210
	(0.667,0.167,0.167)	$= \boldsymbol{w}$	260
Mostly 2	(0.000,1.000,0.000)	$= \boldsymbol{w}$	590
	(0.003,0.993,0.003)	$= \boldsymbol{w}$	575
	(0.017,0.967,0.017)	$= \boldsymbol{w}$	526
	(0.033,0.933,0.033)	$= \boldsymbol{w}$	479
	(0.083,0.833,0.083)	$= \boldsymbol{w}$	398
	(0.167,0.667,0.167)	$= \boldsymbol{w}$	349
Mostly 3	(0.000,0.000,1.000)	$= \boldsymbol{w}$	343
	(0.017,0.017,0.967)	$= \boldsymbol{w}$	369
	(0.033,0.033,0.933)	$= \boldsymbol{w}$	392
	(0.083,0.083,0.833)	$= \boldsymbol{w}$	436
	(0.167,0.167,0.667)	$= \boldsymbol{w}$	422
Mostly 1 and 2	(0.458,0.458,0.083)	$= \boldsymbol{w}$	337
	(0.417,0.417,0.167)	$= \boldsymbol{w}$	327
Mostly 1 and 3	(0.458,0.083,0.458)	$= \boldsymbol{w}$	263
	(0.417,0.167,0.417)	$= \boldsymbol{w}$	299
Mostly 2 and 3	(0.083,0.458,0.458)	$= \boldsymbol{w}$	413
	(0.167,0.417,0.417)	$= \boldsymbol{w}$	380

For the first subpopulation weight scenario, the weights are proportional to sample sizes, with $C_1 = \sum_{x=1}^{3} n_{tx}$ and $C_2 = \sum_{x=1}^{3} n_{t+6,x}$. For all other scenarios, the same subpopulation weights are used at both time points ($\boldsymbol{w} = \boldsymbol{v}$). The (locus averaged) sample sizes at the first time point are $n_{t1} = 30$, $n_{t2} = 9.9$, and $n_{t3} = 9$, whereas at the second time point they are $n_{t+6,1} = 19.5$, $n_{t+6,2} = 9.7$, and $n_{t+6,3} = 19.9$. The realized variance effective sizes $\hat{N}^{\text{int}}_{eVR1} = 155$, $\hat{N}^{\text{int}}_{eVR2} = 590$, and $\hat{N}^{\text{int}}_{eVR3} = 343$ for subpopulations 1,2,3 correspond to values of $\hat{N}^{\text{int}}_{eV\boldsymbol{wv}}$ for the three local weighting schemes $\boldsymbol{w} = \boldsymbol{v} = \boldsymbol{e}_x$, for $x = 1,\ 2,\ 3$

of the estimated subpopulation weighted allele frequencies, in (91), are approximately the same as for homogeneous, binomial samples of sizes n_t and $n_{t+\tau}$.

Table 4 illustrates values of $\hat{N}^{\text{int}}_{eV\boldsymbol{wv}}$ for various choices of subpopulation weights $\boldsymbol{w}$ and $\boldsymbol{v}$. In particular, the local realized variance effective sizes $\hat{N}^{\text{int}}_{eVR1} = 155$, $\hat{N}^{\text{int}}_{eVR2} = 590$, and $\hat{N}^{\text{int}}_{eVR3} = 343$ correspond to choosing local weights $\boldsymbol{w} = \boldsymbol{v} = \boldsymbol{e}_x$ for $x = 1, 2, 3$. It can be seen that the intermediate version of the variance effective population size is maximized for local weights of subpopulation 2, i.e. $\hat{N}^{\text{int}}_{eV\boldsymbol{wv}} = 590$, for $\boldsymbol{w} = \boldsymbol{v} = \boldsymbol{e}_2 = (0, 1, 0)$.

Recall the discussion of Sect. 6.4.2 that equations (55) and (56) are also valid for the intermediate version of the variance effective size, if the system is in migration–drift equilibrium. The findings of Table 4 could therefore indicate that the reproductive weights $\boldsymbol{\gamma}$ are close to $\boldsymbol{e}_2$, so that $N_{eVMeta}^{\text{eq}} = N_{eE}$ is close to $\hat{N}_{eV\boldsymbol{e}_2}^{\text{int}} = 590$. According to Sect. 3, $\gamma = (\gamma_1, \gamma_2, \gamma_3)$ contains the long term genetic contributions from the three subpopulations. If our conclusion $\gamma_2 \approx 1$ is correct, this indicates that $x = 2$ is a source population from which most or all genetic material originates (i.e. unidirectional migration from 2 to 1 and 3). However, for at least two reasons, this is so far only a conjecture: Firstly, more data analysis, with larger sample sizes and more loci, is needed in order to confirm the conclusion that 2 is a source population. Although the JR07-estimator corrects for the sampling effect, the low sample sizes (for $x = 2$ in particular) of this data set indicate that the results of Table 4 are a bit uncertain. A separate analysis, based on the (wrong) assumption that all sample sizes are very large, gives a maximal variance effective size $\hat{N}_{eV\boldsymbol{wv}}^{\text{int}}$ when the three subpopulations are weighted close to uniformly ($w_x = v_x \approx 1/3$ for $x = 1, 2, 3$) at both time points, with a corresponding much lower value of N_{eE}. Secondly, the theoretical results (55) and (56) have only been proved for populations in migration–drift equilibrium, with (55) derived for island models and (56) for models with symmetric migration between subpopulations.

10 Discussion

In this paper we study the variance effective size N_{eV} of a substructured population, with particular focus on the size of the metapopulation (N_{eVMeta}). Our main findings are: (i) That the version of N_{eV} that is of interest for conservation, under certain conditions can be found by maximizing the variance effective size with respect to subpopulation weights in order to minimize the impact of migration and approximate N_{eGD}, (ii) that two new and more stable versions of N_{eV} are introduced and (iii) that the length of the optimal time window of N_{eV}, in terms of estimation accuracy, is derived.

As a major tool for understanding the properties of N_{eV}, we analyze in detail two components of expected squared allele frequency change, defined in equations (21)–(23). The first term I is caused by genetic drift in subpopulations between the two time points at which genetic data is collected, whereas the second term II (or more precisely $-II$) quantifies a correlation between allele frequency change of the past and present. We refer to II as a migration or gene flow term, since it is mainly caused by gene flow between subpopulations, when these are assigned the same weights at both time points at which allele frequencies are estimated from data. General expressions are obtained for how the genetic drift and gene flow terms I and II involve the local census sizes and local effective sizes of subpopulations, the migration pattern between subpopulations and the way in which subpopulations are weighed at the two time points between which genetic change is monitored.

The variance effective size is traditionally defined as in (20), so that expected squared allele frequency change is normalized by its expectation, a normalization that involves allele frequencies at the first time point at which genetic data is collected. We refer to this as the forward version of N_{eV}, since it corresponds to a forward time perspective on how allele frequency change is normalized. As mentioned under (ii), in this article we also introduce, in (25) and (30), two other notions of variance effective size, the intermediate and backward versions of N_{eV}, for which allele frequency change is normalized based on expected allele frequency change at both or only the last time point at which genetic data is collected.

The abovementioned three versions of N_{eV} are very close when the interval between the two time points at which genetic data is collected is small, but they start to differ substantially for intervals with a length that is at least of the same order as the eigenvalue effective size N_{eE}. Two numerical examples are given in this paper in order to illustrate this. The first example represents a large metapopulation with $s = 10$ subpopulations of size 50, for which 200–300 generations are required for the three versions of N_{eV} to differ substantially. The second example represents a small metapopulation with $s = 2$ subpopulations of size 10, for which less than 10 generations is sufficient for the three versions of N_{eV} to differ significantly. We also show that the backward version of N_{eV} is most stable and exists under general conditions, for time intervals of any length. In addition, as mentioned under (iii), we derive in (76), (86), and (90) the length of the optimal time interval for which the forward, intermediate and backward versions of N_{eV} are estimated with maximal accuracy.

As mentioned under (i), a major implication of our work is that the variance effective size of a substructured population, with appropriately chosen subpopulation weights, is relevant for conservation applications. In more detail, let $\hat{N}_{eV\boldsymbol{w}}$ be an estimate of the variance effective size, based on using the same subpopulation weight vector $\boldsymbol{w} = \boldsymbol{v}$ at both time points at which genetic data is collected. We conjecture that

$$\hat{N}_{eE} = \max_{\boldsymbol{w}} \hat{N}_{eV\boldsymbol{w}} \tag{93}$$

is an estimate of the eigenvalue effective size N_{eE} for some population systems close to migration–drift equilibrium. The rationale for (93) is equation (56), which implies that the variance effective size $N_{eV\boldsymbol{w}}$, based on using the same subpopulation weights $\boldsymbol{w} = \boldsymbol{v}$ at both time points at which genetic data is collected, is maximized for reproductive subpopulation weights $\boldsymbol{w} = \boldsymbol{\gamma}$. This follows from the fact that $N_{eV\boldsymbol{w}}$ is maximized when the gene flow term II vanishes, which happens for reproductive subpopulation weights $\boldsymbol{\gamma}$. The conservation relevance of (93) follows from the fact that (a) $N_{eV\boldsymbol{\gamma}}$ is closely related to the gene diversity effective size N_{eGD}, (b) N_{eGD} equals N_{eE} under migration drift equilibrium, and (c) N_{eGD} also approximates the additive genetic variance effective size N_{eAV}, which is of particular interest for long term conservation (Hössjer et al. 2016). Because of the conservation relevance of (93), it is

of interest to develop software that automatically perform the maximization of this equation in order to compute $\hat{N}_{eE}$.

The reproductive weights $\boldsymbol{\gamma}$ depend on the migration pattern between the subpopulations, which typically is unknown. However, equation (93) suggests that it is possible to estimate $\boldsymbol{\gamma}$ indirectly (without first estimating migration rates between subpopulations) as the subpopulation weights that maximize $\hat{N}_{eV_{\boldsymbol{w}}}$. If all subpopulations contribute to the long term reproduction of the metapopulation, all components of $\boldsymbol{\gamma}$ are positive. Whenever this is the case, in order to compute the estimator of N_{eE} in (93), it is required that genetic data is collected from all subpopulations at the two time points between which genetic change is monitored. On the other hand, analysis of the dataset in Sect. 9 indicates that one of the subpopulations might be a source, since the maximum of (93) occurs when this subpopulation is assigned a maximal weight of 1. If this is a correct interpretation of the biological situation, only data from this subpopulation is needed in order to estimate N_{eE}. However, in order to confirm this conclusion a larger dataset is needed, and the validity of (93) must be investigated beyond our present theoretical assumptions (migration–drift equilibrium and symmetric backward migration rates $B_{xy} = B_{yx}$ between all pairs x, y of subpopulations, which implies $\boldsymbol{\gamma} = (1/s, \ldots, 1/s)$) fail.

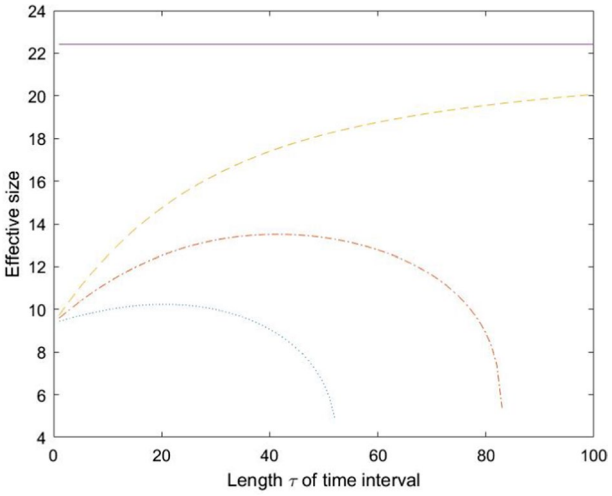

Fig. 5 The figure plots effective sizes for an island model with $s = 2$, $N_{ex} = N_{cx} = 10$ and $m = 0.1$, when $t = 0$ corresponds to migration–drift equilibrium ($T \to \infty$). The horizontal solid line depicts $N_{eE} = 22.42$. The three curves correspond to N_{eVRx} (dotted), N_{eVRx}^{int} (dash-dotted) and N_{eVRx}^{back} (dashed) for intervals $[0, \tau]$ of increasing length. N_{eVRx} increases with τ at first, then it starts to drop until $\tau = \tau_{\max} = 52$, and for longer intervals N_{eVRx} does not exist. In comparison, formula (69) predicts $\tau_{\max,\mathrm{V}} = \log(II_{\infty}^{-1}) \cdot 2N_{eE} = 52.96$. In a similar fashion N_{eVRx}^{int} increases with τ at first, then it starts to drop until $\tau = \tau_{\max} = 83$, and after this generation N_{eVRx}^{int} does not exist. In comparison, formula (71) predicts $\tau_{\max,V}^{\text{int}} = \log(2II_{\infty}^{-1}) \cdot 2N_{eE} = 84.04$. On the other hand, N_{eVRx}^{back} increases monotonically to N_{eE} as $\tau \to \infty$

Several extensions of our work are possible. Firstly, it is possible to investigate whether the present conditions (migration–drift equilibrium and symmetric migration) for equations (56) and (93) can be extended to structured populations of more general form.

Secondly, it is of interest to develop a multilocus estimator of the backward version N_{eV}^{back} of the variance effective size, which analogously to the JR07-estimator of N_{eV}^{int} in Jorde and Ryman (2007) adjusts for finite sampling.

Thirdly, for conservation purposes it is important to study the relation between N_{eV}, N_{eGD}, and N_{eAV} for more general models. We have emphasized that N_{eV}, with reproductive subpopulation weights $\boldsymbol{w} = \boldsymbol{v} = \boldsymbol{\gamma}$, is closely related to N_{eGD} and N_{eAV} (and also with N_{eE} under migration–drift equilibrium). However, this is based on the assumption that N_{eAV} refers to the change of additive genetic variance of a quantitative trait with no epistasis (Hössjer et al. 2016). It is therefore of interest to give more general expressions for N_{eAV} when epistasis is taken into account. We conjecture that N_{eAV} is still very similar to N_{eGD}, and N_{eV} with reproductive weights, for models with epistasis, since all these three effective sizes only involve the drift term I, whereas N_{eV} with other subpopulation weights will be different, since it also involves the correlation term II between past and present allele frequency change.

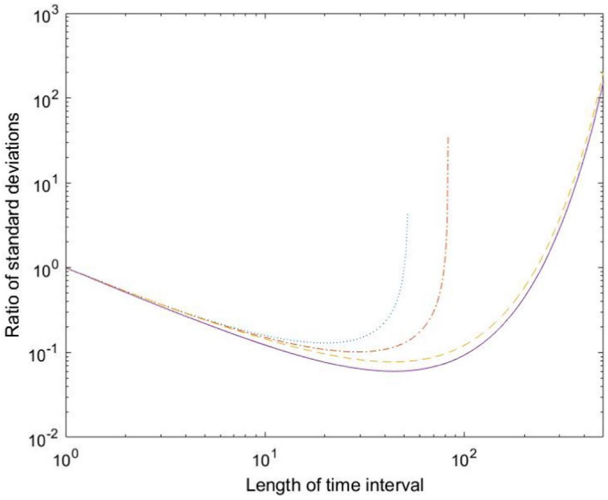

Fig. 6 The figure shows a log–log plot of the normalized standard deviation $\text{Var}\,(\hat{Q})^{1/2}/\sigma$ for estimating $Q = 1/(2N_{eV\boldsymbol{w}}^{\text{method,eq}})$, the average amount of genetic drift per generation at equilibrium, for time intervals $[0, \tau]$. The population is an island model with $s = 2$, $N_{ex} = N_{cx} = 10$, and $m = 0.1$. The dotted, dashed and dashdotted lines correspond to variance effective sizes of a local population ($\boldsymbol{w} = x$), using the forward, intermediate and backward methods respectively, whereas the solid line (the same for all three methods) corresponds to the metapopulation ($\boldsymbol{w} =$ Meta). The optimal time intervals have lengths $\tau_{\text{opt}} = 20$, $\tau_{\text{opt}}^{\text{int}} = 29$, and $\tau_{\text{opt}}^{\text{int}} = 44$ for the local curves of the forward, intermediate and backward methods, and $\tau_{\text{opt,Meta}} = 44$ for the metapopulation. The corresponding approximations are $d_{\text{opt}} 2N_{eE} = 22.24$, $d_{\text{opt}}^{\text{int}} 2N_{eE} = 31.07$, $d_{\text{opt}}^{\text{back}} 2N_{eE} = 44.83$, and $d_{\text{opt,Meta}} 2N_{eE} = 44.83$ respectively. The largest time intervals for which the forward and intermediate effective sizes can be estimated, are $\tau_{\max,V} = 52$ and $\tau_{\max,V}^{\text{int}} = 83$ respectively

A: Appendix with Numerical Examples for a Small and Subdivided Population

In this appendix we demonstrate that sometimes the forward, intermediate, and backward versions of the local realized variance effective size differ substantially for a small and subdivided population, even for time intervals $[0, \tau]$ of moderate (and biologically realistic) lengths.

This is illustrated in Fig. 5 for an island model with $s = 2$ subpopulations of sizes $N_{ex} = N_{cx} = 10$, and a migration rate of $m = 0.1$. It can be seen that the three effective size differ a lot already for $\tau = 5$, with values $N_{eVRx} = 9.71$, $N_{eVRx}^{\text{int}} = 10.39$, and $N_{eVRx}^{\text{back}} = 11.07$, and even more for $\tau = 10$, with values $N_{eVRx} = 9.98$, $N_{eVRx}^{\text{int}} = 11.25$, and $N_{eVRx}^{\text{back}} = 12.51$. The forward and intermediate versions of the realized variance effective size exist for intervals of length up to $\tau = 52$ and 83 generations respectively, whereas the backward version of the realized variance effective exists for intervals of any length.

The corresponding plot of the accuracy of estimates of genetic drift per generation, for intervals of varying length, also reveals a substantial difference between the three versions of variance effective size (cf. Fig. 6).

B: Appendix with Further Numerical Examples and Proofs

B.1: Series Expansion of $\boldsymbol{r}$

We will view the right eigenvector $\boldsymbol{r} = \boldsymbol{r}(\varepsilon)$ of $\boldsymbol{A}$ as a function of $\varepsilon = 1/(2N_{eE})$. Assuming that $0 < N_{eE} \leq \infty$ is large, or equivalently that $\varepsilon \geq 0$ is small, we apply perturbation theory of matrices (Maruyama 1970a; Nagylaki 1980, 1995; Hössjer 2015) in order to find a linear approximation $\boldsymbol{r}(\varepsilon) \approx \boldsymbol{r}(0) + \dot{\boldsymbol{r}}\varepsilon$.

Put $e_x = N_{eE}/N_{ex}$, $c_x = N_{eE}/N_{cx}$ and rewrite the elements of $\boldsymbol{A} = \boldsymbol{A}(\varepsilon)$ in (4) as

$$\begin{aligned} A_{xy,zu}(\varepsilon) &= (1 - c_x\varepsilon)^{1(x=y)} B_{xz} B_{yu} [(1 - e_x\varepsilon)/(1 - c_x\varepsilon)]^{1(z=u)} \\ &\approx A_{xz,yu}(0) + \varepsilon \dot{A}_{xz,yu}, \end{aligned}$$

where

$$A_{xy,zu}(0) = B_{xz} B_{yu} \tag{94}$$

and

$$\dot{A}_{xy,zu} = \big[(c_z - e_z)1(z = u) - c_x 1(x = y)\big] B_{xz} B_{yu}. \tag{95}$$

Note in particular that the two exponents $1(x = y)$ and $1(z = u)$ appear in $A_{xy,zu}(\varepsilon)$ as a consequence of (4). For this reason $A_{xy,zu}(\varepsilon)$ varies with ε, and $\dot{A}_{xy,zu} \neq 0$, only when at least one of the two conditions $x = y$ and $z = u$ is satisfied. It follows from (94) that $\boldsymbol{r}(0) = \mathbf{1}_{s^2} = \mathbf{1}$ is a right eigenvector of $\boldsymbol{A}(0)$ with eigenvalue 1, and therefore

$$\boldsymbol{r}(\varepsilon) \approx \mathbf{1} + \varepsilon \dot{\boldsymbol{r}} + o(\varepsilon) \tag{96}$$

is a valid first order Taylor approximation of $\boldsymbol{r}(\varepsilon)$. In order to find a more explicit expression of $\dot{\boldsymbol{r}}$, we will rewrite it as a linear combination of a system of orthonormal basis functions. To this end, recall that $\boldsymbol{l}_i = (l_{i1}, \ldots, l_{is})$ is a left eigenvector of $\boldsymbol{B}$ with a real-valued eigenvalue η_i, and that $\{\boldsymbol{l}_i\}_{i=1}^{s}$ is an orthonormal system of basis functions for $\mathbb{R}^s$. Define, for each $1 \le i, j \le s$ a row vector $\boldsymbol{l}_{ij} = (l_{ij,xy} = l_{ix} l_{jy}; 1 \le x, y \le s)$ of length s^2. Then $\{\boldsymbol{l}_{ij}; 1 \le i, j \le s\}$ forms an orthonormal system of basis functions for $\mathbb{R}^{s^2}$. We also introduce

$$\xi_{ij} = \boldsymbol{l}_{ij} \dot{\boldsymbol{r}} = \sum_{xy} l_{ij,xy} \dot{r}_{xy} \tag{97}$$

as the coefficient of $\boldsymbol{l}_{ij}^T$ in the basis function expansion

$$\dot{\boldsymbol{r}} = \sum_{ij} \xi_{ij} \boldsymbol{l}_{ij}^T \tag{98}$$

of $\dot{\boldsymbol{r}}$. Since $\boldsymbol{l}_{11} = \mathbf{1}/s$ is proportional to $\boldsymbol{r}(0) = \mathbf{1}$, we may assume that a change from $\varepsilon = 0$ to $\varepsilon > 0$ results in a perturbation $\boldsymbol{r}(\varepsilon) - \boldsymbol{r}(0)$ orthogonal to $\boldsymbol{r}(0)$. This corresponds to an assumption $0 = \xi_{11} = \boldsymbol{l}_{11} \dot{\boldsymbol{r}} = \mathbf{1}^T \dot{\boldsymbol{r}}/s$. In order to find a more explicit expression for all $\{\xi_{ij}; (i,j) \ne (1,1)\}$, we will derive a linear system of equations for the components of $\dot{\boldsymbol{r}} = (\dot{r}_{xy})$, based on an analysis of how $\boldsymbol{r}(\varepsilon)$ is perturbed after small change of ε away from zero. From the definition of ε, and of the eigenvalue effective size in (34), it follows that $\lambda(\varepsilon) = 1 - \varepsilon$. Together with (96), this makes it possible to rewrite $\lambda(\varepsilon)\boldsymbol{r}(\varepsilon) = \boldsymbol{A}(\varepsilon)\boldsymbol{r}(\varepsilon)$ as

$$\begin{aligned} (1-\varepsilon)(\mathbf{1} + \varepsilon \dot{\boldsymbol{r}}) &= (\boldsymbol{A}(0) + \varepsilon \dot{\boldsymbol{A}})(\mathbf{1} + \varepsilon \dot{\boldsymbol{r}}) + o(\varepsilon) \\ &= \mathbf{1} + \varepsilon(\dot{\boldsymbol{A}}\mathbf{1} + \boldsymbol{A}(0)\dot{\boldsymbol{r}}) + o(\varepsilon). \end{aligned} \tag{99}$$

Equating the linear ε-terms of the left- and right-hand sides of (99) we find, after some rearrangements, that

$$\dot{\boldsymbol{r}} - \boldsymbol{A}(0)\dot{\boldsymbol{r}} = \mathbf{1} + \dot{\boldsymbol{A}}\mathbf{1}. \tag{100}$$

Because of (94) and (95), component xy of Eq. (100) takes the form

$$\begin{aligned} \dot{r}_{xy} - \textstyle\sum_{z,u} B_{xz} B_{yu} \dot{r}_{zu} &= 1 + (\dot{\boldsymbol{A}}\mathbf{1})_{xy} \\ &= 1 - c_x 1(x = y) + \textstyle\sum_z (c_z - e_z) B_{xz} B_{yz} \\ &= 1 - c 1(x = y) + (c - e) \textstyle\sum_z B_{xz} B_{yz}, \end{aligned} \tag{101}$$

where the term $1(x = y)$ of the second step is inherited from (95). In the last step of (101) we assumed $N_{ex} = N_e$ and $N_{cx} = N_c$, so that $e_x = e$ and $c_x = c$. Assume that $(i,j) \ne (1,1)$. Multiplying the left and right hand sides of (101) with $l_{ij,xy}$, and summing jointly over x and y, we find, making use of

$$\begin{aligned}\sum_{x,y} l_{ij,xy}\dot{r}_{xy} &= \xi_{ij},\\ \sum_{x,y} l_{ij,xy}B_{xz}B_{yu} &= \eta_i\eta_j l_{ij,zu},\\ \sum_{x,y} l_{ij,xy}B_{xz}B_{yz} &= \eta_i\eta_j l_{ij,zz},\\ \sum_{x,y} l_{ij,xy}1(x=y) &= \sum_x l_{ij,xx} = 1(i=j),\end{aligned}$$

that

$$(1-\eta_i\eta_j)\xi_{ij} = -c1(i=j) + (c-e)\eta_i^2 1(i=j),$$

or equivalently

$$\xi_{ij} = \begin{cases} 1(i=j)\cdot(-c+(c-e)\eta_i^2)/(1-\eta_i^2), & (i,j)\neq(1,1),\\ 0, & (i,j)=(1,1).\end{cases} \tag{102}$$

B.2: Proof of Equation (43)

Inserting (96) into (42) we find that

$$\begin{aligned}F_{ST}^{\text{eq}} &\approx \Big(\sum_{x,y} w_x w_y \dot{r}_{xy} - \sum_x w_x \dot{r}_x\Big)\varepsilon\\ &= -s^{-1}\sum_x \dot{r}_x\cdot\varepsilon\\ &= -s^{-1}\sum_{ij}\xi_{ij}\boldsymbol{l}_i\boldsymbol{l}_j^T\cdot\varepsilon\\ &= s^{-1}\sum_{i=2}^{s}[c-(c-e)\eta_i^2]/(1-\eta_i^2)\cdot\varepsilon\\ &= s^{-1}\sum_{i=2}^{s}[1/N_c-(1/N_c-1/N_e)\eta_i^2]/[2(1-\eta_i^2)],\end{aligned} \tag{103}$$

where in the second step of (103) we used $\boldsymbol{w}=\boldsymbol{\gamma}=\mathbf{1}_s/s$ and the fact that $\sum_{xy}\dot{r}_{xy}=\xi_{11}=0$. In the third step of (103) we inserted the series expansion (98) of $\dot{\boldsymbol{r}}$, in the fourth step we utilized (102), and in the final step we invoked the definitions of $c=N_{eE}/N_c$, $e=N_{eE}/N_e$, and $\varepsilon=1/(2N_{eE})$. This completes the proof since the right hand side of (103) agrees with (43).

B.3: Proof of Equation (48)

In order to prove (48) we will utilize the series expansion of $\boldsymbol{r}$ (or $\dot{\boldsymbol{r}}$). As a first step we need to express $II_\infty(\tau)$ in terms of $\dot{\boldsymbol{r}}$. Insertion of (96) into (47) yields

$$II_\infty(\tau) \approx 2\sum_{x,y}\left[(\boldsymbol{v}\boldsymbol{B}^\tau)_x - w_x\right]w_y\dot{r}_{xy}\cdot\varepsilon. \tag{104}$$

Since $\kappa_i=\boldsymbol{w}\boldsymbol{l}_i^T$ and $\rho_i=\boldsymbol{v}\boldsymbol{l}_i^T$ by assumption, it follows that the analogue of (104), without the factor 2 and with $l_{ij,xy}$ in place of $\dot{r}_{xy}$, reads

$$\begin{aligned}\sum_{xy}\left[(\boldsymbol{v}\boldsymbol{B}^{\tau})_x - w_x\right]w_y \cdot l_{ij,xy} &= \sum_x \left[(\boldsymbol{v}\boldsymbol{B}^{\tau})_x - w_x\right]l_{ix} \cdot \sum_y w_y l_{jy} \\ &= (\eta_i^{\tau}\rho_i - \kappa_i)\kappa_j.\end{aligned} \tag{105}$$

Inserting (98) and (105) into (104) we find that

$$II_{\infty}(\tau) \approx 2 \sum_{(i,j)\neq(1,1)} (\eta_i^{\tau}\rho_i - \kappa_i)\kappa_j \xi_{ij} \cdot \varepsilon. \tag{106}$$

Then we insert the expression (102) for ξ_{ij}, that was derived in Appendix B.1, into (106). This yields

$$\begin{aligned}II_{\infty}(\tau) &\approx 2\sum_{i=2}^{s}(\eta_i^{\tau}\rho_i - \kappa_i)\kappa_i \tfrac{-c+(c-e)\eta_i^2}{1-\eta_i^2} \cdot \varepsilon \\ &= 2\sum_{i=2}^{s} \tfrac{\kappa_i(\kappa_i - \rho_i\eta_i^{\tau})}{1-\eta_i^2}\left[(1-\eta_i^2)c + \eta_i^2 e\right] \cdot \varepsilon.\end{aligned} \tag{107}$$

By substituting the definitions of $\varepsilon = 1/(2N_{eE})$, $c = N_{eE}/N_c$ and $e = N_{eE}/N_e$ into (107) we finally arrive at (48).

B.4: Proofs of Equations (55) and (56)

Recall that Eq. (55) stipulates that the variance effective size at equilibrium, for the island model, is maximized when the same subpopulation weights are used at time points t and $t+\tau$ ($\boldsymbol{w} = \boldsymbol{v}$). Equation (56), on the other hand, is a claim that whenever the same subpopulation weights are used at both time points ($\boldsymbol{w} = \boldsymbol{v}$), the variance effective size at equilibrium is maximized for reproductive subpopulation weights ($\boldsymbol{w} = \boldsymbol{v} = \boldsymbol{\gamma}$). In order to prove these claims we will make use of (52), which states that the variance effective size N_{eV}^{eq} under equilibrium is a strictly decreasing function of the equilibrium gene flow term $II_{\infty}(\tau)$ of Eq. (47). That is, we need to translate (55) and (56) into analogous inequalities for the equilibrium gene flow term in (47). To this end, we will highlight that this term is a function of the weight vectors $\boldsymbol{w}$ and $\boldsymbol{v}$ at time points t and $t+\tau$. More specifically, we will write $II_{\infty}(\tau) = II_{\infty\boldsymbol{w}\boldsymbol{v}}(\tau)$ and $II_{\infty\boldsymbol{w}}(\tau) = II_{\infty\boldsymbol{w}\boldsymbol{w}}(\tau)$. Then, in order to prove (55) it suffices to establish that

$$II_{\infty\boldsymbol{w}\boldsymbol{v}}(\tau) \geq II_{\infty\boldsymbol{w}}(\tau) \tag{108}$$

for the island model whenever $\boldsymbol{w}\boldsymbol{v}^T \leq |\boldsymbol{w}|^2$, with equality in (108) if and only if $\boldsymbol{w}\boldsymbol{v} = |\boldsymbol{w}|^2$. And in order to establish (56) it suffices to prove that

$$II_{\infty\boldsymbol{w}}(\tau) \geq II_{\infty\boldsymbol{\gamma}}(\tau) = 0, \tag{109}$$

for the symmetric migration models of Example 1, with equality if and only if $\boldsymbol{w} = \boldsymbol{\gamma}$. But (108) follows immediately from (49), whereas (109) is deduced from (48) with $\kappa_i = \rho_i$ (since $\boldsymbol{w} = \boldsymbol{v}$ is assumed), and the fact that $\boldsymbol{w} = \boldsymbol{\gamma}$ if and only if $\kappa_2 = \ldots = \kappa_s = 0$.

Acknowledgements The authors wish to thank the handling editor and two reviewers for valuable suggestions that considerably improved the quality of the manuscript. Financial support from the Swedish

Research Council Formas (Grant 2020-01290), the Swedish Research Council (Grant 2019-05503), the Carl Trygger and the Erik Philip-Sörensen Foundations to LL is gratefully acknowledged.

Funding Open access funding provided by Stockholm University.

Declarations

Conflict of interest The authors have no financial interest or other types of conflict of interest related to the work of this article.

Ethical approval The authors guarantee that no study-specific approval from an ethics committee is needed for this work.

Informed consent The authors guarantee that no informed consent is needed for this work.

References

Allendorf FW, Funk WC, Aitken SN, Byrne M, Luikart G (2022) Conservation and the genetics of populations, 3rd edn. Oxford University Press, Oxford

Andersson A, Karlsson S, Ryman N, Laikre L (2022) Mapping and monitoring genetic diversity of an alpine freshwater top predator by applying newly proposed indicators. Mol Ecol 31:6422–6439

Bhatia G, Patterson N, Sankararaman S, Price AL (2013) Estimating and interpreting F_{ST}: the impact of rare variants. Genome Res 23:1514–1521

Cockerham CC (1969) Variance of gene frequencies. Evolution 23:72–84

Crow JF (1954) Breeding structure of populations. II. Effective population number. In: Kempthorne O, Bangcroft TA, Gowen JW, Lush LJ (eds) Statistics and mathematics in biology. Iowa State College Press, Ames, pp 543–566

Crow JF, Kimura M (1970) An introduction to population genetics theory. The Blackburn Press, Caldwell

Durrett R (2008) Probability models for DNA sequence evolution, 2nd edn. Springer, New York

Ewens WJ (1982) On the concept of effective population size. Theor Popul Biol 21:373–378

Ewens WJ (2004) Mathematical population genetics. I. Theoretical introduction, 2nd edn. Springer, New York

Falush D, Stephens M, Pritchard J (2003) Inference of population structure using multilocus genotype data: linked loci and correlated allele frequencies. Genetics 164(4):1567–1587

Frankham R (2021) Suggested improvements to proposed genetic indicator for CBD. Conserv Genet. https://doi.org/10.1007/s10592-021-01357-v

Frankham R, Ballou JD, Briscoe DA (2010) Introduction to conservation genetics, 2nd edn. Cambridge University Press, Cambridge

Frankham R, Bradshaw CJA, Brook BW (2014) Genetics in conservation management: revised recommendations for the 50/500 rules, Red List criteria and population viability analyses. Biol Conserv 170:56–63

Frankham R et al (2019) A practical guide for genetic management of fragmented animal and plant populations. Oxford University Press, Oxford, Online Appendix 2. http://www.oup.co.uk/companion/FrankhamPG

Franklin IR (1980) Evolutionary change in small populations. In: Soule ME, Wilcox BA (eds) Conservational biology: an evolutionary-ecological perspective. Sinauer Associates, Sunderland, pp 135–150
Friswell MI (1996) The derivatives of repeated eigenvalues and their associated eigenvectors. Trans ASME 118:390–397
Gilbert KJ, Whitlock MC (2015) Evaluating methods for estimating local effective population size with and without migration. Evolution 69(8):2154–2166
Hill WG (1972) Effective size of populations with overlapping generations. Theor Popul Biol 3:278–289
Hoban S, Bunford MW, Funk WC, Galbusera P, Griffith MP, Grueber CE, Heuertz M, Hunter ME, Hvilsom C, Kalamujic SB, Kershaw F, Khoury FC, Laikre L, Lopes-Fernandez M, MacDonald AJ, Mergeay J, Meek M, Mittan C, Mukassabi TA, O'Brien D, Ogden R, Palma-Silva C, Ramakrishnan U, Segelbacher G, Shaw RE, Sjögren-Gulve P, Velkovic N, Vernesi C (2021) Global commitments of conserving and monitoring genetic diversity are now necessary and feasible. BioScience. https://doi.org/10.1093/biosci/biab054
Horn RA, Johnson CR (1985) Matrix analysis. Cambridge University Press, Cambridge
Hössjer O (2014) Spatial autocorrelation for subdivided populations with invariant migration schemes. Methodol Comput Appl Probab 16(4):777–810
Hössjer O (2015) On the eigenvalue effective size of structured populations. J Math Biol 71:595–646
Hössjer O, Ryman N (2014) Quasi equilibrium, variance effective size and fixation index for populations with substructure. J Math Biol 69(5):1057–1128
Hössjer O, Jorde PE, Ryman N (2013) Quasi equilibrium approximations of the fixation index under neutrality: the finite and infinite island models. Theor Popul Biol 84:9–24
Hössjer O, Olsson F, Laikre L, Ryman N (2014) A new general analytical approach for modeling patterns of genetic differentiation and effective size of subdivided populations over time. Math Biosci 258:113–133
Hössjer O, Laikre L, Ryman N (2016) Effective sizes and time to migration–drift equilibrium in geographically subdivided populations. Theor Popul Biol 112:139–156
Jamieson IG, Allendorf FW (2012) How does the 50/500 rule apply to MVPs? Trends Ecol Evol 27:578–584
Jorde PE, Ryman N (2007) Unbiased estimator for genetic drift and effective population size. Genetics 177:927–935
Kimbras CB, Tsakas S (1971) The genetics of Dacus oleae. V. Changes of esterase polymorphism in natural population following insecticide control—selection or drift? Evolution 25:454–460
Kimura M (1953) 'Stepping stone' model of population. Annu Rep Natl Inst Genet Jpn 3:62–63
Kimura M, Weiss GH (1964) The stepping stone model of population structure and the decrease of genetic correlation with distance. Genetics 61:763–771
Laikre L, Olsson F, Jansson E, Hössjer O, Ryman N (2016) Metapopulation effective size and conservation genetic goals for the Fennoscandic wolf population. Heredity 117:279–289
Luikart G, Cornuet J-M, Allendorf FW (1999) Temporal changes in allele frequencies provide estimates of population bottleneck size. Conserv Biol 13(3):523–530
Malécot G (1948) Les mathématiques de l'hérédié. Masson & Cie, Paris
Malécot G (1951) Un treatment stochastique des problemès linairés (mutation, linkage, migration) en géneétique de populations. Annales de l'Université de Lyon A 14:79–117
Maruyama T (1970a) On the rate of decrease of heterozygosity in circular stepping stone models of populations. Theor Popul Biol 1:101–119
Maruyama T (1970b) Effective number of alleles in subdivided populations. Theor Popul Biol 1:273–306
Nadachowska-Brzyska K, Konczal M, Babik W (2022) Navigating the temporal continuum of effective population size. Methods Ecol Evol 13:22–41
Nagylaki T (1980) The strong-migration limit in geographically structured populations. J Math Biol 9:101–114
Nagylaki T (1995) The inbreeding effective population number in dioecious populations. Genetics 139:473–485
Nagylaki T (2000) Geographical invariance and the strong-migration limit in subdivided populations. J Math Biol 41:123–142
Nei M (1973) Analysis of gene diversity in subdivided populations. Proc Natl Acad Sci USA 70:3321–3323
Nei M (1977) *F*-statistics and analysis of gene diversity in subdivided populations. Ann Hum Genet 41:225–231
Nei M, Tajima F (1981) Genetic drift and estimation of effective population size. Genetics 98:625–640

Olsson F, Laikre L, Hössjer O, Ryman N (2017) GESP: a computer program for modeling genetic effective population size, inbreeding, and divergence in substructured populations. Mol Ecol Resour 17:1378–1384
Pérez-Pereira N, Wang J, Quesada H, Caballero A (2022) Prediction of the minimum effective size of a population viable in the long term. Biodivers Conserv. https://doi.org/10.1007/s10531-022-02456-z
Pollack E (1983) A new method for estimating the effective population size from allele frequency changes. Genetics 104:531–548
Pritchard JK, Stephens M, Donnelly P (2000) Inference of population structure using multilocus genotype data. Genetics 155:945–959
Richards C, Leberg PL (1996) Temporal changes in allele frequencies and a population's history of severe bottlenecks. Conserv Biol 10:832–839
Rousset F (2004) Genetic structure and selection in subdivided populations. Princeton University Press, Princeton
Ryman N, Allendorf FW, Jorde PE, Laikre L, Hössjer O (2014) Samples from subdivided populations yield biased estimates of effective size that overestimate the rate of loss of genetic variation. Mol Ecol Resour 14:87–99
Ryman N, Laikre L, Hössjer O (2019) Do estimates of contemporary effective population size tell us what we want to know? Mol Ecol 28:1904–1918
Ryman N, Laikre L, Hössjer O (2023) Variance effective population size is affected by census size in substructured populations. Mol Ecol Resour 23:1334–1347. https://doi.org/10.1111/1755-0998.13804
Traill LW, Brook BW, Frankham RR, Bradshaw CJA (2010) Pragmatic population viability targets in a rapidly changing world. Biol Conserv 143:28–34
Tufto J, Hindar K (2003) Effective size in management and conservation of subdivided populations. J Theor Popul Biol 222:273–281
Tufto J, Engen S, Hindar K (1996) Inferring patterns of migration from gene frequencies under equilibrium conditions. Genetics 144:1911–1921
Van der Aa NP, Ter Morsche HG, Mattheij RRM (2007) Computation of eigenvalue and eigenvector derivatives for a general complex-valued eigensystem. Electron J Linear Algebra 16:300–314
Wang J (2016) A comparison of single-sample estimators of effective population sizes from genetic marker data. Mol Ecol 25(19):4692–4711
Waples RS (1989) A generalized approach for estimating effective population size from temporal changes in allele frequency. Genetics 121:379–391
Waples RS (2016) Making sense of genetic estimates of effective population size. Mol Ecol 25(19):4689–4691
Weir BS, Cockerham CC (1984) Estimating *F*-statistics for the analysis of population structure. Evolution 38:1468–1476
Weiss GH, Kimura M (1965) A mathematical analysis of the stepping stone model of genetic correlation. J Appl Probab 2:129–149
Whitlock MC, Barton NH (1997) The effective size of a subdivided population. Genetics 146:427–441
Wright S (1931) Evolution in Mendelian populations. Genetics 16:97–159
Wright S (1938) Size of population and breeding structure in relation to evolution. Science 87:430–431
Wright S (1943) Isolation by distance. Genetics 28:114–156
Wright S (1949) The general structure of populations. Ann Eugen 15:323–354

Authors and Affiliations

Ola Hössjer[1] · Linda Laikre[2] · Nils Ryman[2]

✉ Ola Hössjer
ola@math.su.se

Linda Laikre
linda.laikre@popgen.su.se

Nils Ryman
nils.ryman@popgen.su.se

[1] Division of Mathematical Statistics, Department of Mathematics, Stockholm University, 106 91 Stockholm, Sweden

[2] Division of Population Genetics, Department of Zoology, Stockholm University, 106 91 Stockholm, Sweden